

Bowdoin College

Bowdoin Digital Commons

Physics Faculty Publications

Faculty Scholarship and Creative Work

4-12-1993

Simple-current symmetries, rank-level duality, and linear skein relations for Chern-Simons graphs

Stephen G. Naculich
Johns Hopkins University

Harold A. Riggs
Brandeis University

Howard J. Schnitzer
Brandeis University

Follow this and additional works at: <https://digitalcommons.bowdoin.edu/physics-faculty-publications>

Recommended Citation

Naculich, Stephen G.; Riggs, Harold A.; and Schnitzer, Howard J., "Simple-current symmetries, rank-level duality, and linear skein relations for Chern-Simons graphs" (1993). *Physics Faculty Publications*. 157.
<https://digitalcommons.bowdoin.edu/physics-faculty-publications/157>

This Article is brought to you for free and open access by the Faculty Scholarship and Creative Work at Bowdoin Digital Commons. It has been accepted for inclusion in Physics Faculty Publications by an authorized administrator of Bowdoin Digital Commons. For more information, please contact mdoyle@bowdoin.edu, a.sauer@bowdoin.edu.

Simple-current symmetries, rank–level duality, and linear skein relations for Chern–Simons graphs *

Stephen G. Naculich ^{1,b}, Harold A. Riggs ^a and Howard J. Schnitzer ^a

^a *Department of Physics, Brandeis University, Waltham, MA 02254, USA*

^b *Department of Physics and Astronomy, The Johns Hopkins University, Baltimore, MD 21218, USA*

Received 20 May 1992

Accepted for publication 28 September 1992

A previously proposed two-step algorithm for calculating the expectation values of arbitrary Chern–Simons graphs fails to determine certain crucial signs. The step which involves calculating tetrahedra by solving certain non-linear equations is repaired by introducing additional linear equations. The step which involves reducing arbitrary graphs to sums of products of tetrahedra remains seriously disabled, apart from a few exceptional cases. As a first step towards a new algorithm for general graphs we find useful linear equations for those special graphs which support knots and links. Using the improved set of equations for tetrahedra we examine the symmetries between tetrahedra generated by arbitrary simple currents. Along the way we describe the simple, classical origin of simple-current charges. The improved skein relations also lead to exact identities between planar tetrahedra in level K $G(N)$ and level N $G(K)$ Chern–Simons theories, where $G(N)$ denotes a classical group. These results are recast as WZW braid-matrix identities and as identities between quantum $6j$ -symbols at appropriate roots of unity. We also obtain the transformation properties of arbitrary graphs, knots, and links under simple-current symmetries and rank–level duality. For links with knotted components this requires precise control of the braid eigenvalue permutation signs, which we obtain from plethysm and an explicit expression for the (multiplicity-free) signs, valid for all compact gauge groups and all fusion products.

1. Introduction

Topologically invariant Chern–Simons gauge theories in $2 + 1$ dimensions are interacting – yet completely soluble – quantum field theories [1]. Quantization of such a theory with compact gauge group G forces the coupling constant K to be an integer. The fixing of these integer values of K leads to the appearance of discrete symmetries associated with automorphisms of the extended Dynkin diagram for G [2], as well as remarkable relations between those models with a classical group $G(N)$ as gauge group and coupling constant K and those with gauge group $G(K)$

* Supported in part by the DOE under grant DE-FG02-92ER40706

¹ Supported in part by the NSF under grant PHY-90-96198

and coupling constant N [3]. While the presence of these symmetries in several contexts has long been known [4–6], only recently have the pervasive implications of these symmetries for Chern–Simons theories [3,7], integrable lattice models [8,9], and quantum groups [9] begun to be studied *. In much of this existing work the effects of these discrete symmetries have been derived only for restricted cases. For the extended Dynkin diagram automorphisms (which signal the presence of simple-current symmetries in the associated WZW model [4]) the properties of the modular transformation matrix have been of central interest [5,10–13]. This corresponds in Chern–Simons theory only to the expectation values of the simplest knot, the unknot, and the simplest link, two linked unknots (the Hopf link) [1]. Similarly, although the rank–level duality of the characteristic polynomial of the braid matrix or its spectral decomposition holds for many tensor representations of the groups involved, this result only leads to a duality of expectation values for special classes of knots or links [3,7]. The analogous results for the associated quantum groups and lattice models [8,9], which have proceeded by explicit construction of the quantities involved, have only been obtained for restricted classes of representations: the completely symmetric and antisymmetric representations of $SU(N)$. Our goal in this paper is to attain an exact, general result, without restrictions on the representations or classes of links involved.

The advantage of examining this question in the context of three-dimensional Chern–Simons theory is that, in addition to providing a powerful and unifying approach to almost all the different areas in which these discrete symmetries appear, it provides the tools with which to demonstrate the general implications of these symmetries without having to explicitly solve for the quantities being related.

Of special interest are certain gauge invariant Chern–Simons observables: the planar tetrahedra. This follows since all Chern–Simons observables can be expressed as sums of products of these tetrahedra [11,14]. They are also the q -6j-symbols of the related quantum groups evaluated at the associated roots of unity. In addition, the planar tetrahedra are related by simple phases to limiting values of the Boltzmann weights of integrable lattice models and to the braid matrices of WZW theory [1].

Our strategy will be to examine sets of skein relations that completely determine the expectation values of arbitrary tetrahedra. A previously proposed set of non-linear skein relations [14] suffers from a sign ambiguity that renders them ineffective for the exact determination of all tetrahedra. We will remove this ambiguity by supplementing these non-linear equations with a set of inhomogeneous linear equations. We are then able to show that given any tetrahedron there

* The general idea that Wilson lines with representations related by the Dynkin diagram symmetries are equivalent up to phases has long been known [2], however, and has been used to understand Chern–Simons theories with gauge groups of the form $G/(\text{discrete subgroup})$.

exists a class of tetrahedra, related to this one by the symmetries of the extended Dynkin diagram of the gauge group, whose expectation values only differ from that of the original tetrahedron by (in general, vertex-normalization dependent) signs. If the tetrahedral expectation values are intrinsic (i.e. independent of the sign convention for vertex normalization), then the relative sign is given by a certain product of braid eigenvalues. We further show that given a tetrahedron in one theory, there are tetrahedra in the rank-level dual theory with the same expectation values (up to sign). If the signs of the tetrahedra so related are intrinsic, the relative sign is again given by a simple product of braid eigenvalues.

Since arbitrary observables in a $G(N)_K$ Chern–Simons theory (including knots, links and graphs) can be reduced to sums of products of tetrahedra, we expect that all such observables will fall into sets related by the Dynkin diagram automorphisms, and have, in addition, rank-level duals in the $G(K)_N$ theory. A general proof along these lines is stymied by the presence of certain undetermined, *normalization-independent* signs in most such reductions. Nevertheless, on the basis of cases where an unambiguous reduction is possible and on the basis of the properties of the linear equations which we obtain for any link-type graph, we state the expected general result for such graphs for both types of symmetry. Identities between knot and link expectation values defined with representations related by the diagram automorphisms can be proved via a direct cabling argument; the aforementioned identities for the underlying link-type graphs then follow. The identities that relate knot and link expectation values in rank-level dual theories are shown to follow from the conjectured identities between dual graphs.

Our approach only deals with the local, Lie-algebraic structure of Chern–Simons theory; to avoid conflicts with global constraints [15] we assume that each theory is defined with a compact, connected, and simply connected gauge group. This is appropriate since such Lie groups are in one-to-one correspondence with (complex) Lie algebras (and so with the standard set of Dynkin diagrams). For example, in order to obtain a theory with the local structure of B_n or D_n with arbitrary coupling constant K , and in order to include their spinor representations, it must be defined via the simply connected covering group of $SO(N)$, $Spin(N)$. Since it will be useful (in sect. 4, essential) to characterize these theories using the tensorial language of the orthogonal group we will refer to these theories as level K $so(N)$ theories (by which we mean level $2K$ $Spin(N)$ theories) *.

In sect. 2 we describe the known non-linear equations for tetrahedra and find the supplemental equations that remove the sign ambiguity of the non-linear set. We pay particular attention to the permutation signs appearing in the diagonal action of the braid matrix on the legs of trivalent vertices and the normalization of

* The (non-simply connected) level K $SO(N)$ theory is defined by the level $2K$ $Spin(N)/\mathbb{Z}_2$ theory, given appropriate restrictions on K .

these vertices, in order to deal uniformly with real, pseudoreal, and complex representations. We adopt a natural system of permutation signs different from that commonly prescribed in the literature. In sect. 3 we show that replacing the representations around a closed loop of edges of a tetrahedron with representations related to these by simple-current symmetries leaves the tetrahedral expectation value essentially invariant. We will call the tetrahedra (or representations) so related co-minimally equivalent [3,7]. In sect. 4 we find that, given a tetrahedron in a $G(N)_K$ theory, with $G(N)$ denoting $SU(N)$, $Sp(N)$, or the double-cover of $SO(2n+1)^*$, and with the representations on its edges specified by Young tableaux, the tetrahedra in the $G(K)_N$ theory with edge representations specified by the transposes (or certain cominimal equivalents of the transposes) of these Young tableaux have essentially the same expectation value. In sect. 5 these results are recast as identities for WZW fusion and braid matrices as well as for the q -6j-symbols appearing in quantum group [16] theory. In sect. 6, we examine more general graphs and the knots and links based on them. We give a simple, graph-independent, and completely general derivation of the phases that relate links (or knots) with co-minimally equivalent representations on corresponding components. We state (and give evidence for, but do not prove) identities that we expect to hold between arbitrary Chern–Simons observables related by rank–level duality.

The appendix following the conclusion describes certain subtleties of baryon normalization, a proof of a useful identity by means of plethysm, and several other results on permutation signs needed in the text, including an explicit formula for these signs in the multiplicity-free case, valid for all compact gauge groups and all fusion products.

2. Tetrahedral skein relations: A sign problem and its solution

We shall see later that a previously proposed algorithm for calculating arbitrary Chern–Simons observables [14] suffers from sign ambiguities that render it ineffective for evaluating general graphs and links. However, the part of this algorithm that involves solving certain non-linear (associativity or pentagon) equations for planar tetrahedra is repairable, which is the task of the present section. Along the way we give a more comprehensive account of the permutation signs that arise in the diagonal action of the braid matrix than has previously appeared, and take account of certain subtleties of baryon normalization.

We begin with a level K Chern–Simons theory with compact, connected, and simply connected gauge group G defined on the 3-manifold $M = S^3$. Since G is

* Similar but more complicated results hold for dual pairs involving $so(2n)$; we will not, however, present the details here. As a result we only examine rank–level duality for $so(2n+1)_K$ with K odd.

simply connected, G-bundles over M are trivial and the theory is well defined by the action [15]

$$S_{\text{CS}} = \frac{K}{4\pi} \text{Tr} \int (A \wedge dA + \frac{2}{3} A \wedge A \wedge A), \quad (2.1)$$

where A is the G gauge connection, and quantization forces K to be an integer. In order for the partition function

$$Z(S^3) = \int \mathcal{D}A \, e^{iS_{\text{CS}}} \quad (2.2)$$

to be unambiguously defined it must be regularized by specifying a framing [17] of S^3 . We choose this framing [17] so that $Z(S^3) = S_{00}$, where S_{00} is the identity–identity component of the modular transformation matrix of the level K characters of the affinization of G. The gauge invariant observables \mathcal{O} , whose expectation values are given by

$$Z(\mathcal{O}; S^3) = \int \mathcal{D}A \, e^{iS_{\text{CS}} \mathcal{O}}, \quad (2.3)$$

correspond to linked – often knotted – Wilson lines and graphs. To obtain an unambiguous definition of these expectation values we will assume throughout a vertical framing of the Wilson lines and graphs [1]. We will be concerned exclusively with the normalized expectation values,

$$\langle \mathcal{O} \rangle = \frac{Z(\mathcal{O}; S^3)}{Z(S^3)}. \quad (2.4)$$

Among the graph observables are those specified by single-component planar graphs with four trivalent gauge-invariant vertices – the planar tetrahedra. Any tetrahedron corresponds to a pair of fusion-rule channels, with each channel defined by a pair of compatible fusion rules. These channels come in natural sets of three which, following ref. [14], we call the S , T , and U channels. Each of these channels corresponds to a basis of the Hilbert space on which some braid matrix acts diagonally. The compatibility of these bases gives a set of equations that constrain the basis change coefficients, which are, essentially, the expectation values of planar tetrahedra.

2.1. S , T AND U CHANNEL BASES

Choose a surface S^2 that divides S^3 into two halves (call one the interior half; the other, the exterior), in such a way that it is punctured at exactly four points by static charges, corresponding to the four representations a , b , $\rho(c)$ and $\rho(d)$ of

$G(N)$. (For the groups we are considering, the dual representation $\rho(r)$ of r is just the representation conjugate to r .) The Hilbert space \mathcal{H} associated with this surface, considered as the boundary of the interior half of S^3 , exists and is $f = \sum_s N_{ab}^s N_{cd}^s$ dimensional whenever the pair of fusion rules

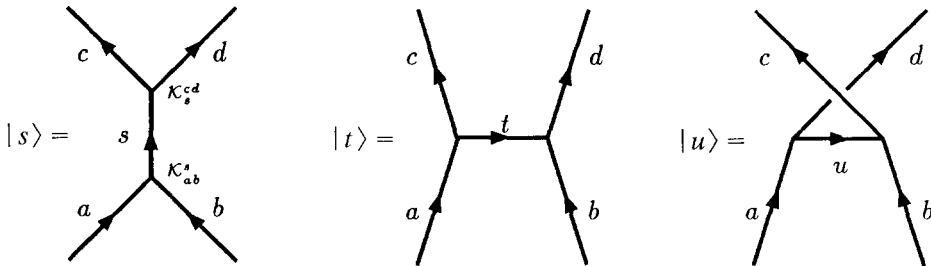
$$\phi_a \cdot \phi_b = \sum_s N_{ab}^s \phi_s, \quad \phi_c \cdot \phi_d = \sum_s N_{cd}^s \phi_s, \quad (2.5)$$

has some representation in common (i.e. whenever $f \neq 0$). Such a pair of fusion rules will be called *compatible*. The path integral on the interior half can produce a variety of states in \mathcal{H} depending on how the Wilson lines or graphs intertwine in the interior. We will consider the relation between three different planar bases of this space, corresponding to the three sets of compatible fusion rule pairs

$$\begin{array}{lll} \text{S-channel} & \text{T-channel} & \text{U-channel} \\ \phi_a \cdot \phi_b = \sum_s N_{ab}^s \phi_s, & \phi_a \cdot \phi_{\rho(c)} = \sum_t N_{a\rho(c)}^t \phi_t, & \phi_a \cdot \phi_{\rho(d)} = \sum_u N_{a\rho(d)}^u \phi_u, \\ \phi_c \cdot \phi_d = \sum_s N_{cd}^s \phi_s, & \phi_{\rho(b)} \cdot \phi_d = \sum_t N_{\rho(b)d}^t \phi_t, & \phi_{\rho(b)} \cdot \phi_c = \sum_u N_{\rho(b)c}^u \phi_u. \end{array} \quad (2.6)$$

Each non-zero fusion coefficient $N_{r_1 r_2}^{r_3}$ corresponds to a set of $N_{r_1 r_2}^{r_3}$ gauge invariant couplings, each of which permits construction of a gauge invariant trivalent vertex. In order to describe the properly framed graphs that specify the bases of \mathcal{H} constructed with these vertices, we must keep track of the (here vertical) framing. This is done by a generic projection of the graph onto a plane and a restriction to certain allowed moves [18] in manipulating the resulting diagrams – the standard Chern–Simons link and graph moves [1].

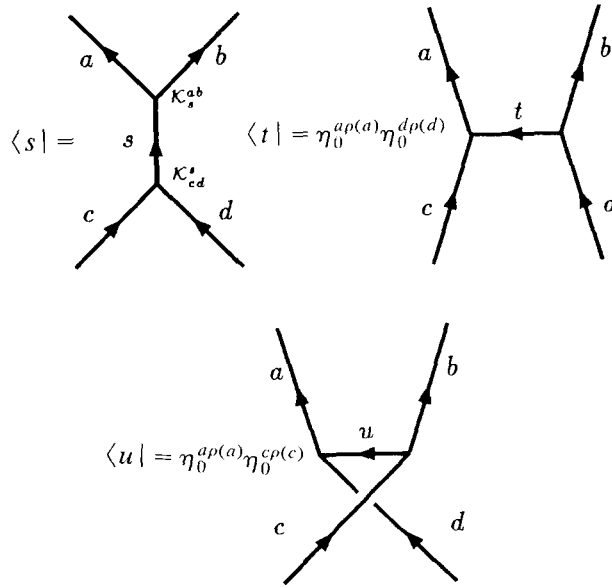
Then, with the bases defined by



each of these channels corresponds to an f -dimensional basis of the Hilbert space \mathcal{H} . We will denote the basis vectors in the various channels by a single label $|s\rangle$, $|t\rangle$, or $|u\rangle$ where, for example, $|s\rangle = |ab \rightarrow cd; s, \mathcal{K}_{ab}^s, \mathcal{K}_s^{cd}\rangle$ denotes the vector created by the path integral in the presence of the S-channel graph shown above, with \mathcal{K}_{ab}^s and \mathcal{K}_s^{cd} used to couple the representations associated with the graph

edges. Upper indices on a coupling indicate outgoing edge arrows at the vertex; lower indices, incoming edge arrows. (For visual clarity, we will mostly omit explicit display of these couplings on graph vertices.)

We assume that a basis of couplings can be chosen so that the relevant braid matrices act diagonally even in the case of multiplicities. The bases defined above then have the dual bases



The permutation signs $\eta_0^{r\rho(r)} = \pm 1$ appearing here result from the signs of certain baryon expectation values (as described in the appendix and subsect. 2.2) and insure that these states satisfy the orthonormalizations

$$\langle s' | s \rangle = \delta_{s's} \chi_q(a) \chi_q(b) \chi_q(c) \chi_q(d) > 0, \quad (2.7)$$

where $\chi_q(r)$ denotes the q -dimension of the representation r . The delta function means that the *entire* intermediate channel, as specified by a representation and a pair of couplings, must be dual. Thus $|s\rangle$ is orthogonal to $|s'\rangle$ unless the intermediate representation is the same, *and* unless the couplings at each vertex are the same, in the basis chosen above ^{*}.

2.2. PERMUTATION SIGNS AND BARYONS

Associated with each planar basis of \mathcal{H} is a pair of braid operators that act diagonally on the basis vectors by interchanging adjacent vertex legs of the basis

^{*} I.e. since dual couplings satisfy $\mathcal{K}_s^{ab}(i)\mathcal{K}_{ab}^s(i') \propto \delta_{ii'}$ with $i, i' = 1, \dots, N_{ab}^s$, this means, unless $i = i'$.

vector graphs. For example, the action of the braid operator B_{ab} on the dual S-channel vectors is specified by

$$B_{ab} \begin{array}{c} a \quad b \\ \diagdown \quad \diagup \\ \quad \quad c \\ \uparrow \end{array} = \varrho_c^{ab} \begin{array}{c} b \quad a \\ \diagdown \quad \diagup \\ \quad \quad c \\ \uparrow \end{array} \quad (2.8)$$

where the diagonal matrix elements (which we will loosely call “eigenvalues”) are

$$\varrho_c^{ab} = \eta_c^{ab} q^{(Q(a)+Q(b)-Q(c))/4} \quad \text{with} \quad q = e^{2\pi i/(K+\bar{g})}. \quad (2.9)$$

Here $\eta_c^{ab} = \pm 1$ is the Chern–Simons permutation sign, \bar{g} is the dual Coxeter number of G , and $Q(r) = 2(K + \bar{g})h(r)$ with $h(r)$ the conformal weight of the level K representation of the affinization of G specified by r . For the simple, compact gauge groups considered in depth here $Q(r)$ is the quadratic Casimir of the representation r . We will specify all braid eigenvalues with reference to the specific edge orientations shown in (2.8) so that ϱ_c^{ab} always corresponds to $c \in a \otimes b$ and the quadratic Casimir of the lower-index representation always enters with a minus sign (as in eq. (2.9)). On the other hand, we will adopt an index convention for η_c^{ab} that keeps track of edge orientations: the same index convention as that of the coupling \mathcal{K}_c^{ab} ; namely, that upper (lower) indices imply outgoing (incoming) arrows.

Several of the results in sect. 3 hold for Chern–Simons theories with more general compact gauge groups, such as those corresponding to various rational conformal field theories. In these cases, $Q(\phi) = 2(K + \bar{g})h(\phi)$ with $h(\phi)$ the conformal weight of the primary field ϕ of the associated conformal field theory. In addition, eqs. (2.28)–(2.34) hold as identities between quantum 6j-symbols (using the connection with planar tetrahedra given in sect. 5) with the braid eigenvalues given by eq. (2.9) but with q not necessarily a root of unity.

The permutation signs require careful consideration in order to give a consistent treatment in all cases, including that of groups with pseudoreal representations. They satisfy the identity

$$\mathcal{P}^{ab} \mathcal{K}_c^{ab} = \eta_c^{ab} \mathcal{K}_c^{ba}, \quad (2.10)$$

where $\mathcal{P}^{ab}: V^a \otimes V^b \rightarrow V^b \otimes V^a$ is the permutation operator. If $a = b$ the sign η_c^{aa} is independent of the normalization sign ω of the coupling \mathcal{K}_c^{aa} and only depends on the embedding of the representation c in the tensor product $a \otimes a$. If $a \neq b$, however, η_c^{ab} is fixed by the choice of the relative sign of the normalization signs ω_1 of the coupling \mathcal{K}_c^{ab} and ω_2 of the permuted coupling \mathcal{K}_c^{ba} . We will refer to the normalization independent signs η_s^{aa} as the *intrinsic* permutation signs. Once a consistent system of permutation signs is chosen there still remains a single undetermined sign ω for each triple $\{a, b; c\}$ related by $a \otimes b \ni c$. Baryon normal-

ization fixes the normalization $\bar{\omega}$ of the dual couplings \mathcal{K}_{ab}^c in terms of the sign ω chosen for \mathcal{K}_c^{ab} , so that for each set $\{\mathcal{K}_c^{ab}, \mathcal{K}_c^{ba}, \mathcal{K}_{ab}^c, \mathcal{K}_{ba}^c\}$ there remains just one undetermined residual sign ω (whether $a = b$ or not).

Throughout this paper, the sign of any expectation value will be called *intrinsic* or vertex-normalization independent, if, given a system of permutation signs and baryon normalizations, it is independent of the choice of these residual normalization signs. Note that the word “intrinsic” is being used for two slightly different concepts.

We can make any choice of the relative sign of the normalizations ω_1 and ω_2 for a particular set of couplings, and so any choice for η_c^{ab} with $a \neq b$, that we wish. However, in order to obtain a consistent set of topologically meaningful graphical moves with which to manipulate the planar projections of knot, link, and graph observables with *arbitrary* representations, certain constraints on these signs must be satisfied. In the appendix we find that, given the standard normalization of baryons, the following three conditions must be satisfied if we are to retain the standard graphical moves for graphs with arbitrary representations on their edges.

1. $\eta_c^{ab} = \eta_{\rho(b)}^{a\rho(c)}$ crossing,
2. $\eta_{\rho(c)}^{\rho(a)\rho(b)} = \eta_c^{ab}$ conjugation,
3. $\eta_0^{c\rho(c)} = \eta_0^{a\rho(a)}\eta_0^{b\rho(b)}$ for $c \in a \otimes b$ fusion. (2.11)

(Here, and throughout, 0 denotes the identity representation.) While we have singled out these three constraints, the use of eq. (A.9) to reduce vertices with orientations other than that of eq. (2.8) to this standard form (before acting with B_{ab}) leads to various other crossing constraints of the form $\eta_c^{ab} = \eta^{ab\rho(c)} = \eta_{\rho(a)\rho(b)c} = \dots$, so that we need only (and will only) refer to the standard form η_c^{ab} .

An immediate consequence of the fusion constraint in (2.11) is that the charge conjugation signs must satisfy (with $r(a)$ denoting the number of boxes of the tableau a)

$$\eta_0^{a\rho(a)} = \left(\eta_0^{\square\rho(\square)}\right)^{r(a)} \quad \text{all classical groups,}$$

$$\eta_0^{(\psi;a)\rho((\psi;a))} = \eta_0^{\psi\rho(\psi)}\eta_0^{a\rho(a)} \quad \text{so}(N), \quad (2.12)$$

for all tensor representations a and spin representations $\{\psi; a\}$ with tensor part a . The fundamental spinor is denoted by ψ , and \square denotes the fundamental tensor representation. A further useful consequence of the fusion constraint in (2.11) for a compatible fusion rule channel (as in eq. (2.6)) is that $\eta_0^{a\rho(a)}\eta_0^{b\rho(b)} = \eta_0^{c\rho(c)}\eta_0^{d\rho(d)}$.

The common (manifestly crossing-symmetric) proposal that η_c^{ab} be uniformly chosen positive in the cases with $a \neq b$, $\rho(c) \neq a$, and $\rho(c) \neq b$ (simultaneously), cannot be adopted here, since it runs afoul of the fusion constraint in (2.11) as follows. Consider $SU(N)$ with $N = (2 \times \text{odd number})$, i.e. the unitary groups with

pseudoreal representations. Then, with a denoting the pseudoreal representation specified by a single column of $N/2$ boxes, we necessarily have, from the first equation in (2.12), that

$$\eta_0^{\square \rho(\square)} = \eta_0^{aa} = -1, \quad (2.13)$$

even though $\eta_0^{\square \rho(\square)}$ is not an intrinsic sign, since $\square \neq \rho(\square)$ unless $N = 2$. The first identity in (2.12) then fixes the charge conjugation signs of all representations whose tableaux have an odd number of boxes (only a fraction of which are connected by crossing to an intrinsic sign) to be negative. Therefore, the first identity in (2.12) leads to a series of counter-examples to the “positive if not connected by crossing to an intrinsic sign” prescription.

The other well-known system of permutation signs, the standard $SU(2)$ group theory signs

$$\epsilon_{j_3}^{j_1 j_2} = (-1)^{j_1 + j_2 - j_3}, \quad (2.14)$$

cannot be directly used in $SU(2)$ Chern–Simons theory since they do not, in fact, obey the crossing constraint listed in (2.11).

A crossing-symmetric system of signs that also obeys the fusion constraint can, however, be directly obtained in terms of a certain, natural system of group theory signs. The group theory signs are defined by

$$\mathcal{P}^{ab} \mathcal{C}_c^{ab} = \epsilon_c^{ab} \mathcal{C}_c^{ba}, \quad (2.15)$$

where \mathcal{C}_c^{ab} is the transpose of the matrix of Clebsch–Gordan coefficients $\mathcal{C}_{ab}^c : V_a \otimes V_b \rightarrow V_c$. Again, if $a = b$ these signs are intrinsic but if $a \neq b$ we may choose them at will. There is, however, a natural choice for these latter signs. In ref. [19] this natural sign system is obtained for all compact, simple Lie groups and all tensor products. The centerpiece for this system is a general formula for ϵ_c^{ab} (in terms of the highest-weight vectors of the representations a , b , and c alone) in the case where c occurs in the tensor product $a \otimes b$ with no multiplicity

$$\epsilon_c^{ab} = (-1)^{(\lambda | a + b - c)/2} \quad (\text{no multiplicity}). \quad (2.16)$$

Here λ is the level vector for the group G (defined by the condition that $(\lambda | \alpha) = 1$ for all simple roots α of G)*. (Since $\lambda = \alpha$ for $SU(2)$, eq. 2.14 turns out to be a particular case of eq. 2.16.) The problems that arise in the case of multiplicities are discussed in the appendix. This is a *natural* system of signs in the sense that ϵ_c^{ab} originates in the structure of the embedding of c in the tensor product $a \otimes b$ for $a \neq b$ in exactly the same way that the sign ϵ_c^{aa} originates in the embedding of c in

* If α is long, we set $(\alpha | \alpha) = 2$, in which case the level vector differs from the sum of positive roots only if G is non-simply laced.

$a \otimes a$ (as shown in ref. [19] and illustrated in the appendix), and corresponds to the choice of normalization $\omega_1 = \omega_2 = \omega$ (with ω a residual, undetermined sign).

This natural system of group theory signs satisfies the identities

$$\begin{aligned} 1. \quad \epsilon_c^{ab} &= \epsilon_{\rho(b)}^{a\rho(c)} \epsilon_0^{a\rho(a)} && \text{crossing,} \\ 2. \quad \epsilon_{\rho(c)}^{\rho(a)\rho(b)} &= \epsilon_c^{ab} && \text{conjugation,} \\ 3. \quad \epsilon_0^{c\rho(c)} &= \epsilon_0^{a\rho(a)} \epsilon_0^{b\rho(b)} \quad \text{for } c \in a \otimes b && \text{fusion.} \end{aligned} \quad (2.17)$$

The first identity shows that these signs do not satisfy the crossing constraint on the Chern–Simons signs in eq. (2.11) when $\epsilon_0^{a\rho(a)}$ is negative.

While this natural system of permutation signs is not crossing symmetric, the modified system given by

$$\eta_c^{ab} = \epsilon_c^{ab} \epsilon_0^{c\rho(c)} = (-1)^{(\lambda|a+b+c)/2} \quad (\text{no multiplicity}), \quad (2.18)$$

does provide a consistent crossing-symmetric sign system for Chern–Simons theory that satisfies all the constraints of (2.11).

Since the fusion identity in eq. (2.17) implies that $\epsilon_0^{c\rho(c)} = 1$ if $a = b$ (i.e. if $c \in a \otimes a$), the *intrinsic* Chern–Simons permutation signs equal the *intrinsic* group-theory signs, as is well known. Since this fusion identity also implies that $\epsilon_0^{00} = 1$, eq. (2.18) also equates the Chern–Simons charge conjugation signs $\eta_0^{a\rho(a)}$ with the (natural) group theory signs $\epsilon_0^{a\rho(a)}$.

2.3. THE NATURAL CHARGE CONJUGATION SIGNS

Since the natural charge conjugation signs $\eta_0^{a\rho(a)}$ appear pervasively, and since they often necessarily differ from the common expectation that only pseudoreal representations require a negative charge conjugation sign, we exhibit their values in detail. These signs are given – in all cases since the identity always appears with multiplicity one – by eq. (2.18), which reduces to

$$\eta_0^{a\rho(a)} = (-1)^{(\lambda|a)} \quad (2.19)$$

in this case since $(\lambda|a) = (\lambda|\rho(a))$. In most cases these signs are actually completely determined by the fusion constraint (or in any case fixed by being either intrinsic or related by the fusion constraint to an intrinsic sign) so that there is actually little freedom of choice in Chern–Simons theory for these signs.

Since $\square = \rho(\square)$ for $\mathfrak{so}(N)$ and $\mathfrak{Sp}(N)$, we must have $\eta_0^{\square\rho(\square)} = 1$ for $\mathfrak{so}(N)$ (which also follows necessarily from the fusion constraint) and $\eta_0^{\square\rho(\square)} = -1$ for

$\mathrm{Sp}(N)$ (which does not). Then eq. (2.12) requires, in agreement with eq. (2.19), that

$$\eta_0^{a\rho(a)} = \begin{cases} 1 & \mathrm{so}(N) \\ (-1)^{r(a)} & \mathrm{Sp}(N), \end{cases} \quad (2.20)$$

for all tensor representations a^* . For $\mathrm{so}(8n+4 \pm 1)$ ($\mathrm{so}(8n+4)$) with $n = 0, 1, \dots$ the fundamental spinor(s) is(are) pseudoreal. Since $\eta_0^{\psi\rho(\psi)} = -1$ in these cases, eqs. (2.12) and (2.20) then imply that the charge conjugation sign is necessarily negative for all spin-tensor representations $\{\psi; a\}$ of these groups. However, for $\mathrm{so}(8n+6)$ the fundamental spinors are complex and we choose (though this is not required by eq. (2.11)) the charge conjugation sign to be -1 in accordance with eq. (2.19).

For G_2 , F_4 , E_6 and E_8 , the Chern–Simons constraints in eq. (2.11) alone fix all charge conjugation signs to be positive. For E_6 this represents a constraint beyond pure group theory, since the fundamental representation is complex. For E_7 the charge conjugation sign of the fundamental is necessarily negative since this representation is pseudoreal. While this fixes all other charge conjugation signs via eqs. (2.11), these are all self-conjugate and so intrinsic.

For $\mathrm{SU}(N)$ the natural sign for the fundamental is $\eta_0^{\square\rho(\square)} = (-1)^{N-1}$. In fact, if $N = (\text{odd number})$ the fusion constraint forces $\eta_0^{\square\rho(\square)} = 1$, since the number of boxes modulo two is not conserved by the tensor ring. As noted previously, if $N = (2 \times \text{odd number})$ then we must set $\eta_0^{\square\rho(\square)} = -1$ due to the fusion constraint in (2.11). On the other hand, for $N = (2 \times \text{even number})$ the natural sign for the fundamental (which is negative) is not intrinsic and not required by the fusion constraint. We will adopt – for all values of N – the natural system for the charge conjugation signs, so that

$$\eta_0^{a\rho(a)} = (-1)^{(N-1)r(a)} \quad \mathrm{SU}(N), \quad (2.21)$$

for all representations a .

In table 1 we summarize these results. In all cases the representations a with $\eta_0^{a\rho(a)} = 1$ form a closed (sub)ring. The fusion constraint alone actually forces the positive value on this (sub)ring. In most other cases the fusion constraint connects the charge conjugation sign of the remaining representations to an intrinsic sign. The (remaining free) choice of the signs for the fundamental representation of $\mathrm{SU}(4n)$ and the fundamental spinors of $\mathrm{so}(4n+2)$ then leaves all signs fixed. Note

* Only for the (complex) tensor representations of $\mathrm{so}(4n+2)$ with self-associate Young tableaux is eq. (2.20) a constraint beyond that required by pure group theory.

TABLE 1

Group	$\eta_0^{a\rho(a)}$
$SU(2n), Sp(N)$	$(-1)^{r(a)}$
$SU(2n+1)$	1
G_2, F_4, E_6, E_8	1
E_7	$\begin{cases} \text{real} & 1 \\ \text{pseudoreal} & -1 \end{cases}$
$SO(N_+)$	1
$SO(N_-)$	$\begin{cases} \text{tensors} & 1 \\ \text{spinors} & -1 \end{cases}$
$N_+ = \{7, 8, 9, 10\} + 8n$ and	
$N_- = \{3, 4, 5, 6\} + 8n$ with $n = 0, 1, \dots$	

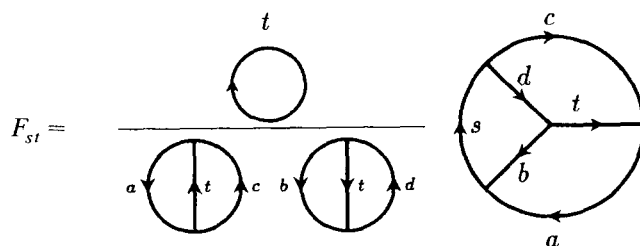
that the appearance of minus signs is (necessarily) not restricted to the pseudoreal case.

2.4. NON-LINEAR SKEIN RELATIONS FOR PLANAR TETRAHEDRA

Since the vectors $|s\rangle, |t\rangle, |u\rangle$ (defined in subsect. 2.1) form different bases of the same space, we can expand any given basis vector in terms of the other bases.

$$\begin{aligned}
 |s\rangle &= \sum_t F_{st} |t\rangle, \\
 |s\rangle &= \sum_u (\varrho_s^{cd})^{-1} G_{su} |u\rangle, \\
 |t\rangle &= \sum_u (\varrho_a^{tc})^{-1} \varrho_{\rho(u)}^{\rho(c)b} H_{tu} |u\rangle.
 \end{aligned} \tag{2.22}$$

The entries in the $f \times f$ matrices F , G , and H are just the expectation values of planar tetrahedra



$$\begin{aligned}
 G_{su} = & \begin{array}{c} \text{Diagram 1: A circle with a vertical line through its center. The left half is labeled 'a' and the right half 'd'. The top half is labeled 'u' and the bottom half 'c'. The edges are oriented: 'a' points down, 'd' points up, 'u' points right, 'c' points left.} \\ \text{Diagram 2: A circle with a vertical line through its center. The left half is labeled 'a' and the right half 'c'. The top half is labeled 'u' and the bottom half 'd'. The edges are oriented: 'a' points down, 'c' points up, 'u' points right, 'd' points left.} \end{array} \\
 H_{tu} = & \begin{array}{c} \text{Diagram 3: A circle with a vertical line through its center. The left half is labeled 'a' and the right half 'c'. The top half is labeled 'u' and the bottom half 'd'. The edges are oriented: 'a' points down, 'c' points up, 'u' points right, 'd' points left.} \\ \text{Diagram 4: A circle with a vertical line through its center. The left half is labeled 'a' and the right half 'c'. The top half is labeled 'u' and the bottom half 'd'. The edges are oriented: 'a' points down, 'c' points up, 'u' points right, 'd' points left.} \end{array}
 \end{aligned}
 \tag{2.23}$$

Note that the edge orientations on the baryons imply (via eq. (A.14)) the possible presence of minus signs in the baryon expectation values.

Explicit calculation of the inverse transformations along with the orthogonality and completeness of the three bases shows that the matrices of tetrahedra satisfy [14]

$$\begin{aligned}
 FF^T &= I, & FF^\dagger &= I, \\
 GG^T &= I, & GG^\dagger &= I, \\
 HH^T &= I, & HH^\dagger &= I.
 \end{aligned}
 \tag{2.24}$$

From these equations one concludes that F , G and H are real matrices. Written out, the remaining independent equations for these real matrices are

$$\sum_s F_{st} F_{st'} = \delta_{tt'}, \quad \sum_u G_{su} G_{s'u} = \delta_{ss'}, \quad \sum_t H_{tu} H_{tu'} = \delta_{uu'}. \tag{2.25}$$

These constitute $3f(f+1)/2$ equations for $3f^2$ real unknowns and so do not by themselves contain enough information to solve for the tetrahedra. The associativity of the basis change operations (2.22) gives the further set of equations [14]

$$F_{st} = \sum_u \left(\varrho_s^{cd} \varrho_t^{ap(c)} \varrho_u^{\rho(b)c} \mathcal{F}_c^{-1} \right) G_{su} H_{tu}, \tag{2.26}$$

where $\mathcal{F}_c = q^{Q(c)/2}$ is the vertical-framing factor incurred in undoing a self-cross-

ing of a Wilson line carrying the representation c . This equation and its complex conjugate provide $2f^2$ further constraints, so that we have in general more constraints than unknowns. These conditions ostensibly overdetermine the tetrahedra, given that no unforeseen degeneracies in the braid eigenvalues occur [14].

However, eqs. (2.25) and (2.26) have certain discrete symmetries, a fact which is both necessary and problematic. For if we have generic tetrahedra (a , b , c and d all different), then changing the residual normalization ω of the coupling \mathcal{K}_s^{ab} at the common vertex connecting a , b and s in F_{st} and G_{su} , for example, will change the sign of a row of F_{st} and of G_{su} , but the non-linear equations will remain unchanged. Since these equations hold for arbitrary tetrahedra, they must allow for and not determine this sign ambiguity, since this is entirely a matter of the arbitrary choice of sign of the vertex normalization. However, certain tetrahedra have intrinsic signs which are then not determined by these equations even though their signs are independent of vertex normalization. Primary among these latter tetrahedra are the *link-type* tetrahedra, which have $d = a$ and $c = b$:

Here the vertices occur in dual pairs whose relative normalization is fixed once the permutation signs and baryon normalization are fixed. Therefore a change of residual vertex normalization cancels and does not affect the overall sign of such link-type tetrahedra. Since this sign is intrinsic and since the non-linear equations cannot determine it we need a further prescription that will enable the calculation of these intrinsic signs.

2.5. LINEAR SKEIN RELATIONS FOR PLANAR TETRAHEDRA

The problem of determining the signs of link-type tetrahedra that remain unfixed by the (non-linear) orthogonality and associativity equations is solved by appeal to the following inhomogeneous linear equations. While they are special cases of the general construction valid for all link-type graphs described in sect. 6, they also follow directly from the definitions of the tetrahedra in eq. (2.22). By acting with B_{ab} and B_{ab}^{-1} on the expansion of $|s\rangle$ in terms of $|t\rangle$, and vice versa,

we obtain, from the braid closure of the resulting diagrams, the 4f equations for the f^2 quantities F_{st}

$$\begin{aligned}
 & \text{Diagram 1: A circle with a vertical line through the center. The left half has an arrow pointing down, labeled 'a'. The right half has an arrow pointing up, labeled 'b'. The top half has an arrow pointing right, labeled 's'.} \quad (\varrho_s^{ab})^{\pm 1} = \sum_t F_{st} (\varrho_t^{a\rho(b)})^{\mp 1} \quad \text{Diagram 2: A circle with a vertical line through the center. The left half has an arrow pointing down, labeled 'b'. The right half has an arrow pointing up, labeled 'a'. The top half has an arrow pointing right, labeled 't'.} \\
 & \text{Diagram 3: A circle with a vertical line through the center. The left half has an arrow pointing down, labeled 'b'. The right half has an arrow pointing up, labeled 'a'. The bottom half has an arrow pointing right, labeled 's'.} \quad (\varrho_t^{a\rho(b)})^{\pm 1} = \sum_s F_{st} (\varrho_s^{ab})^{\mp 1} \quad \text{Diagram 4: A circle with a vertical line through the center. The left half has an arrow pointing down, labeled 'a'. The right half has an arrow pointing up, labeled 'b'. The bottom half has an arrow pointing right, labeled 't'.} \quad (2.28)
 \end{aligned}$$

From the results of subsect. 2.2 and the appendix we find that

$$\frac{\text{Diagram 1}}{\text{Diagram 3}} = \eta_0^{b\rho(b)} \sqrt{\frac{\chi_q(s)}{\chi_q(t)}} \quad (2.29)$$

Then the equations in (2.28) can be written in the form

$$\begin{aligned}
 (\varrho_s^{ab})^2 \sqrt{\chi_q(s)} &= \sum_t (\eta_0^{b\rho(b)} \varrho_s^{ab} F_{st} \varrho_t^{a\rho(b)}) \sqrt{\chi_q(t)} (\varrho_t^{a\rho(b)})^{-2}, \\
 (\varrho_t^{a\rho(b)})^2 \sqrt{\chi_q(t)} &= \sum_s (\eta_0^{b\rho(b)} \varrho_s^{ab} F_{st} \varrho_t^{a\rho(b)}) \sqrt{\chi_q(s)} (\varrho_s^{ab})^{-2} \quad (2.30)
 \end{aligned}$$

(or, using the fact that the F_{st} are real, in the form of the complex conjugates of these equations). For the following, the quantity

$$\eta_0^{b\rho(b)} \varrho_{s_i}^{ab} F_{s_i t_j} \varrho_{t_j}^{a\rho(b)} \quad (2.31)$$

will then be of prime interest. The non-linear equations (2.25) and (2.26) determine the absolute value of F_{st} ; the linear equations (2.28) fix the remaining sign ambiguity. The signs of the link-type tetrahedra F_{st} clearly depend on the choice of a system of permutation signs and baryon normalizations. However, from eq. (2.30) it is seen that the quantity in eq. (2.31) only depends on the *squares* of braid eigenvalues and on the q -dimensions. It not only does not depend on the residual vertex normalization signs; it also does not depend on any choice of a particular system of permutation signs.

If we think of the freedom to choose the vertex normalization (and so the permutation signs) as a local, discrete gauge symmetry (in which guise it does

appear in integrable lattice models) then the product of tetrahedra and eigenvalues in eq. (2.31) is a natural gauge invariant quantity.

In sect. 5 we shall see that the expressions in (2.31) are essentially the non-planar tetrahedra that equal the matrix elements of a class of WZW braid matrices.

For $f = 1, 2, 3$ and 4 the equations in (2.28) alone determine F_{st} , and an explicit general solution for all link-type tetrahedra is possible in these cases without appeal to the non-linear equations.

For $f = 1$ one finds that

$$F_{st} = \eta_0^{b\rho(b)} \sqrt{\frac{\chi_s}{\chi_t}} Q_s^{ab} Q_t^{a\rho(b)}. \quad (2.32)$$

Since $\chi_t = \chi_s$ when $f = 1$, this simplifies to

$$F_{st} = \eta_0^{b\rho(b)} Q_s^{ab} Q_t^{a\rho(b)} \quad (f = 1). \quad (2.33)$$

In addition, the non-linear, orthogonality condition (2.25) yields $F_{st} = \pm 1$ for all tetrahedra if $f = 1$. Therefore, we must have $Q_s^{ab} Q_t^{a\rho(b)} = (Q_s^{ab} Q_t^{a\rho(b)})^{-1} = \pm 1$, which constrains the values of the quadratic Casimirs appearing in an $f = 1$ fusion rule.

For $f = 2$, with an arbitrary ordering of the two terms in each of the fusion rules $\phi_a \cdot \phi_b = \phi_{s_1} + \phi_{s_2}$ and $\phi_a \cdot \phi_{\rho(b)} = \phi_{t_1} + \phi_{t_2}$, we find that

$$F_{s_1 t_1} = \eta_0^{b\rho(b)} \sqrt{\frac{\chi_{s_1}}{\chi_{t_1}}} Q_{s_1}^{ab} Q_{t_1}^{a\rho(b)} \frac{1 - (Q_{s_1}^{ab})^{-2} (Q_{t_2}^{a\rho(b)})^{-2}}{1 - (Q_{t_1}^{a\rho(b)})^2 (Q_{t_2}^{a\rho(b)})^{-2}} \quad (f = 2). \quad (2.34)$$

In these solvable cases we see explicitly that F_{st} is a rational function of braid eigenvalues with an overall sign that depends in a complicated way on the permutation signs, baryon normalization, and the form of this function. In contrast, the quantity in (2.31) is a rational function of the *squares* of the braid eigenvalues and does not depend on the system of permutation signs or the baryon normalization. While its value depends on the values of the Casimirs and the structure of this function, this information is just that encoded in the structure of eq. (2.30). The same will be true for any f by appeal to the whole system of non-linear and linear equations (except that an explicit solution of these equations will not be generally available). This means that the symmetries of this combined set of equations will be exact symmetries of the combination $\eta_0^{b\rho(b)} Q_{s_i}^{ab} F_{s_i t_j} Q_{t_j}^{a\rho(b)}$ for all consistent choices of permutation signs and baryon normalization.

Although a special case, the link-type tetrahedra are important because they are the only tetrahedra that directly support knot and link invariants. They will also be important in sect. 6 where their special properties lead to proofs of certain identities for more complex graphs.

Since the combined skein relations in eqs. (2.25), (2.26) and (2.30) are maximally effective for the exact determination of all tetrahedra, we can now explore the symmetries between tetrahedra by examining the transformation properties of the fusion coefficients, quadratic Casimirs, and permutation signs appearing as coefficients of eqs. (2.26) and (2.30).

3. Simple currents, co-minimal equivalence, and planar tetrahedra

The fusion ring of a level K WZW model based on any simple, compact Lie group G arises as a quotient of the classical tensor ring of G by a certain ideal. Such a fusion ring has automorphisms of the form

$$N_{\sigma^m(a)\sigma^n(b)}^{\sigma^{m+n}(c)} = N_{ab}^c \quad \text{with} \quad \sigma^p(r) = r \quad \text{for all } r, \quad (3.1)$$

for some positive integer p if and only if the center Z of G is nontrivial – with exactly one exception (the E_8 level-2 fusion ring) [4,20]. Such automorphisms correspond to the presence of a discrete (integer) charge [10] γ that is conserved mod p by the fusion product

$$N_{ab}^c \neq 0 \Rightarrow \gamma(c) = \gamma(a) + \gamma(b) \quad \text{mod } p. \quad (3.2)$$

Curiously, these charges have – as we shall see – a completely classical origin: the classical tensor ring has exactly this mod p conservation law, so that the fusion ring (as a quotient) necessarily inherits the same additive conservation law. Since all known rational fusion rings (those with a finite number of elements) are obtained from these WZW fusion rings by forming further products and quotients and since these automorphisms have profound implications [10] for coset field identifications [2,21], simple-current fixed-point resolution, and the construction of modular invariant partition functions [22], it is of interest to study their exact consequences in the associated Chern–Simons theories.

Given rather general properties of any fusion ring, eq. (3.1) implies the following constraint on the conformal dimensions [10] for an automorphism σ of order p :

$$h(\sigma(a)) = h(a) + h(\sigma(0)) - k(a)/p, \quad (3.3)$$

for some integer $k(a)$ (unknown at this level of generality). If we define

$$\gamma(a) = k(a) \quad \text{mod } p \quad (3.4)$$

then eq. (3.2) is satisfied. It will be useful to define the fractional charge

$q(a) = \gamma(a)/p$ which is conserved mod one *. Since $q(\rho(a)) = -q(a)$ we have the braid eigenvalue identities (from eq. (2.9))

$$\begin{aligned} \mathcal{Q}_{\sigma(s)}^{\sigma(a)b} &= (\pm)_s e^{i\pi q(b)} \mathcal{Q}_s^{ab}, \\ \mathcal{Q}_{\sigma(t)}^{\sigma(a)\rho(b)} &= (\pm)_t e^{-i\pi q(b)} \mathcal{Q}_t^{a\rho(b)}, \end{aligned} \quad (3.5)$$

where the undetermined sign depends on s (or t). In addition, it follows from general constraints and eq. (3.1) that the q -dimensions (given that they are real, linear functions on the fusion ring) must satisfy [10]

$$\chi_q(\sigma(a)) = \chi_q(a). \quad (3.6)$$

Precise results for the transformation properties of the tetrahedral quantity in eq. (2.31), as well as those of linked unknots, will only require the three constraints, eqs. (3.1), (3.5) and (3.6), and will not depend on any choice of a system of permutation signs. Therefore, these results will hold in *any* Chern–Simons theory with simple current symmetries.

In order to obtain analogous results for (linked) *knots*, or to calculate the braid eigenvalues and permutation sign in eq. (2.31), we will need to know the integers $k(a)$ exactly. In addition we will need some understanding of how the permutation signs transform under the fusion rule automorphisms. We provide this level of precision only for Chern–Simons theories with compact, simply-connected gauge groups. In the cases $SU(N)$, $Sp(N)$, $so(2n+1)$, $so(4n+2)$, E_6 and E_7 the center is cyclic and isomorphic to the group generated by a single automorphism σ (of order $p = \dim\{\text{center}\}$) of the extended Dynkin diagram of G which permutes the affine vertex with a vertex of the ordinary Dynkin diagram. For $so(4n)$ the center is isomorphic to the group generated by two independent automorphisms σ_1 and σ_2 each of order two. The elements of the fusion ring are divided into equivalence classes – we call them [3,7] *co-minimal equivalence classes* – by the map between representations associated with the action of the aforementioned diagram automorphism groups.

For the classical groups σ has a natural interpretation in terms of Young tableaux:

$$SU(N)_K$$

σ acts on a reduced tableau a by adding a row of length K to the top of a .
(A tableau is reduced if it has no columns of length N .)

* This charge $q(a)$ is the same fraction ($|q(a)| < 1$) defined in ref. [10] via the leading pole in the conformal block of ϕ_a appearing in an operator product expansion, although there the integer ambiguity is compounded with the question of which field in the conformal block occurs as the leading pole.

$\mathrm{Sp}(N)_K$

$\sigma(a)$ denotes the complement of the tableau a in an $N \times K$ rectangle.

$\mathrm{so}(2n+1)_K$

σ maps a tableau with first row length l_1 to a tableau with first row length $K - l_1$ (but otherwise identical).

$\mathrm{so}(4n)_K$

σ_1 has the same definition as the (tableau) map σ for $\mathrm{so}(2n+1)_K$.

σ_2 denotes the complement of a tableau in an $\frac{1}{2}N \times \frac{1}{2}K$ rectangle (with $N = 4n$) if $l_1 \leq \frac{1}{2}K$ and if $l_{N/2} \geq 0$; in general, $l_i(\sigma_2(a)) + l_{N/2+1-i}(a) = \frac{1}{2}K$.

If K is odd, σ_2 interchanges spinors and tensors.

$\mathrm{so}(4n+2)_K$

$\sigma = \sigma_2 \circ \sigma_1$ is the composition of the two operations just defined for $\mathrm{so}(4n)$ (except that now $N = 4n + 2$ in the definition of σ_2); its order is four.

For the spin-tensors of $\mathrm{so}(2n+1)$ or $\mathrm{so}(2n)$ we add a column of n half-boxes to the Young tableaux in order to implement the operations just described. (Consult the initial paragraphs of the appendix for the translation between Young tableau row lengths, the labels l_i , and Dynkin indices.)

Using the Dynkin numbering for the E_6 diagram, the Dynkin indices of $\sigma(a)$, a_i^σ , are such that $a_1^\sigma = a_0$; the \mathbb{Z}_2 generator σ for E_7 is unambiguous.

The representations related by the action of the groups generated by these maps are usefully termed “co-minimally equivalent” since the quadratic Casimirs (so also the conformal dimensions), fusion coefficients, and q -dimensions have (by explicit verification) the transformation properties:

$$h(\sigma(a)) = \begin{cases} h(a) + \frac{(N-1)K}{2N} - \frac{r(a)}{N} & \text{for } \mathrm{SU}(N) \\ h(a) + \frac{1}{4}NK - \frac{1}{2}r(a) & \text{for } \mathrm{Sp}(N) \\ h(a) + \frac{1}{2}K - l_1(a) & \text{for } \mathrm{so}(2n+1) \text{ and} \\ & \text{so}(4n) \text{ if } \sigma = \sigma_1 \\ h(a) + \frac{1}{16}NK - \frac{1}{2}r(a) & \text{for } \mathrm{so}(4n+2) \text{ and} \\ & \text{so}(4n) \text{ if } \sigma = \sigma_2 \\ h(a) + \frac{1}{3}2K - \frac{1}{3}(2(\kappa|a) + 3I_1) & \text{for } E_6 \\ h(a) + \frac{1}{4}3K - \frac{1}{2}(3(\kappa|a) + 2I_2) & \text{for } E_7, \end{cases}$$

$$N_{\sigma^m(a)\sigma^n(b)}^{\sigma^{m+n}(c)} = N_{ab}^c,$$

$$\chi_q(\sigma(a)) = \chi_q(a). \quad (3.7)$$

Here

$$r(a) = \sum_{i=1}^{\text{rank}\{G\}} l_i(a),$$

and the l_i are given in terms of the Dynkin indices in the appendix. For all representations a of $SU(N)$ or $Sp(N)$, $r(a)$ equals the number of boxes in the associated Young tableaux. For any (tensor or spinor) representation of $so(2n)$ the quantity $r(a)$ and the number of boxes $r^y(a)$ of the diagram of a are related by

$$r(a) = r^y(a) - 2\nu |l_{N/2}(a)|. \quad (3.8)$$

Here ν equals zero (one) if $a_n > a_{n-1}$ ($a_n < a_{n-1}$). The diagram of a spin-tensor $\{\psi; a\}$ is formed by adjoining a column of n half-boxes to the Young tableau for a , so that $r^y(\{\psi; a\}) = r^y(a) + n/2$. While for tensors of $so(N)$ the label l_1 is an integer (the first Young tableau row length), for spin-tensors $\{\psi; a\}$ it is not: $l_1(\{\psi; a\}) = l_1(a) + \frac{1}{2}$. With Dynkin numbering for the E_6 and E_7 Dynkin indices, we have set

$$I_1 = 2a_3 + a_4 + a_6 \quad \text{and} \quad I_2 = a_1 + 2a_2 + 3a_3 + a_4 + a_5.$$

In addition, the product of the (congruence) vector [23] κ with the highest weight of a is explicitly given by $(\kappa|a) = a_1 + 2a_2 + a_4 + 2a_5$ for E_6 , and by $(\kappa|a) = a_4 + a_6 + a_7$ for E_7 .

3.1. THE ORIGIN OF SIMPLE-CURRENT CHARGES

The formulae for $h(\sigma(a))$ provide explicit expressions for the simple current charges. Inspection of these expressions shows that, in all cases of WZW simple currents (apart from E_8 level 2), the simple-current charges γ coincide [10] exactly with the congruence classes of the group G . The congruence class of a representation a of G is given by $(\kappa|a) \bmod p$ (where p is the order of the relevant automorphism generator discussed above and κ is the associated congruence vector). The importance of these classes stems from the fact that, for all $c \in a \otimes b$,

$$(\kappa|c) = (\kappa|a) + (\kappa|b) \bmod p. \quad (3.9)$$

This is the conservation law of the tensor ring that is inherited by the fusion ring. In the case of the classical groups these congruence classes have simple Young tableau interpretations, which clearly indicates their origin in the $GL(N)$ tensor ring.

$SU(N)$

$\gamma(a) = r(a) \bmod N$ distinguishes the well-known N -ality classes.

$Sp(N)$

$\gamma(a) = r(a) \bmod 2$ distinguishes real ($r(a)$ even) from pseudoreal ($r(a)$ odd) representations.

$\mathfrak{so}(2n+1)$

$\gamma(a) = 2l_1(a) \bmod 2$ indicates whether a is a tensor ($l_1(a)$ integer) or spinor ($l_1(a)$ half-integer) representation.

$\mathfrak{so}(4n)$

$\gamma_1(a) = 2l_1(a) \bmod 2$ again distinguishes tensor and spinor representations.

$\gamma_2(a) = r(a) \bmod 2$ indicates whether the number of boxes associated with a tensor representation is even or odd. For spinor representations it indicates whether the number of diagram boxes plus ν is even or odd. (The relation to the standard definition of κ is that $r(a) \bmod 2 = \frac{1}{2}[(\kappa|a) \bmod 4]$ with $(\kappa|a) = 2r(a)$.)

$\mathfrak{so}(4n+2)$

$\gamma(a) = 2r(a) \bmod 4$ differentiates tensors ($\gamma = 0, 2$) with an even ($\gamma = 0$) or odd ($\gamma = 2$) number of boxes from spinors ($\gamma = 1, 3$) with the number of boxes plus ν even or odd.

E_6

$\gamma(a) = 2(\kappa|a) \bmod 3$ coincides with the standard triality classes $\{0, 1, 2\}$, except that the labels 1 and 2 are interchanged.

E_7

$\gamma(a) = 3(\kappa|a) \bmod 2$ coincides with the duality which distinguishes real and pseudo-real representations (except that the labels 0 and 1 are exchanged).

If we define new congruence vectors for E_6 ($\kappa' = 2\kappa$), E_7 ($\kappa' = 3\kappa$) and σ_2 of $\mathfrak{so}(4n)$ ($\kappa'_2 = \frac{1}{2}\kappa_2$) then in all cases

$$\gamma(a) = (\kappa|a) \bmod p. \quad (3.10)$$

For the classical groups we see that all the tensorial charges originate (ultimately) in the exact conservation of the number of Young tableau boxes (i.e. in the fact that $c \in a \otimes b \rightarrow r(a) + r(b) = r(c)$) exhibited by the $GL(N)$ or $U(N)$ tensor rings. In each case the classical tensor ring of G conserves the charge mod a number that reflects how G is defined as a subgroup of $GL(N)$ or $U(N)$. For example, the various mod 2 quantities result from the existence of an invariant tensor that implements contractions of tensor indices two at a time. For the orthogonal groups the charge ν distinguishes the two irreducible representations of $\mathfrak{so}(N)$ that branch from self-associate representations of $O(N)$. The distinction between tensors and spinors is the only additional concept (which can be seen as exact conservation of half boxes).

3.2. PERMUTATION SIGNS AND CO-MINIMAL EQUIVALENCE

The remaining ambiguity in eq. (3.5) arises from the permutation signs. For any given sign η_c^{ab} eq. (2.18) rapidly yields its value if c appears in the tensor product $a \otimes b$ with multiplicity one. Difficulties can arise if one tries to obtain general

formulae from this equation alone because it is difficult to implement the condition of no multiplicities. In the case of $SU(N)$, for example, with

$$\Delta_c^{ab} = \frac{r(a) + r(b) - r(c)}{N}, \quad (3.11)$$

we find (from eq. (2.18)) that

$$\eta_{\sigma(c)}^{\sigma(a)b} = \exp[i\pi(K(N+1) + r(b) + N\Delta_c^{ab})] \eta_c^{ab}, \quad (3.12)$$

if c appears with multiplicity one in the decomposition of $a \otimes b$, and the same for $\sigma(c)$ in $\sigma(a) \otimes b$. The iteration of eq. (3.12) (or direct calculation) in the case $b = \sigma(a)$ and $c = \sigma(s)$ then leads to

$$\eta_{\sigma^2(s)}^{\sigma(a)\sigma(a)} = \exp[i\pi(r(a) + r(\sigma(a)) + N\Delta_s^{aa} + N\Delta_{\sigma(s)}^{a\sigma(a)})] \eta_s^{aa} \quad (SU(N)_K), \quad (3.13)$$

which holds exactly if both s is multiplicity free in $a \otimes a$ and $\sigma^2(s)$ is multiplicity free in $\sigma(a) \otimes \sigma(a)$. If N is odd, then eq. (3.13) depends on the intermediate channel

$$\eta_{\sigma^2(s)}^{\sigma(a)\sigma(a)} = \exp[i\pi(K + l_{N-1}(s))] \eta_s^{aa} \quad (N \text{ odd; multiplicity free}). \quad (3.14)$$

However, exactly this dependence also arises from the transformation of the conformal dimensions (3.7) in the braid eigenvalue so that (in agreement with eq. (3.5))

$$\mathcal{Q}_{\sigma^2(s)}^{\sigma(a)\sigma(a)} = \exp\left[i\pi \frac{N+1}{N} (r(\sigma(a)) + r(a))\right] \mathcal{Q}_s^{aa} \quad (N \text{ odd}) \quad (3.15)$$

holds if both multiplicity free conditions hold. For N even, eq. (3.13) reduces to

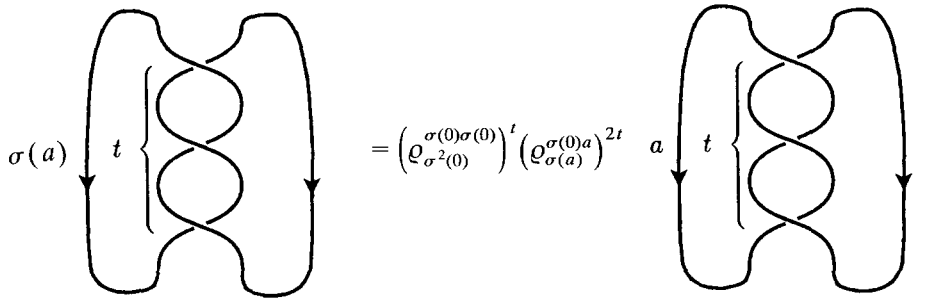
$$\eta_{\sigma^2(s)}^{\sigma(a)\sigma(a)} = e^{i\pi K} \eta_s^{aa} \quad (N \text{ even; multiplicity free}), \quad (3.16)$$

and there is no intermediate channel dependence to cancel that coming from the conformal dimensions. Then, given the multiplicity free conditions,

$$\begin{aligned} \mathcal{Q}_{\sigma^2(s)}^{\sigma(a)\sigma(a)} &= \exp[i\pi(l_{N-1}(a) + l_{N-1}(s))] \\ &\times \exp\left[i\pi \frac{N+1}{N} (r(\sigma(a)) + r(a))\right] \mathcal{Q}_s^{aa} \quad (N \text{ even}) \end{aligned} \quad (3.17)$$

seems to contain some intermediate channel dependence. Despite this appearance, this dependence is spurious. In order to demonstrate this, and to get at the cases

with multiplicity, consider the following. From the (independently proved) result in (6.30) for a trefoil-type knot with an odd number of twists t (with $t = \pm 3$ being the case of the trefoil proper),



$$\sigma(a) \left\{ t \right\} = \left(\varrho_{\sigma^2(0)}^{\sigma(0)\sigma(0)} \right)^t \left(\varrho_{\sigma(a)}^{\sigma(0)a} \right)^{2t} a \left\{ t \right\} \quad (3.18)$$

we obtain

$$\sum_s N_{\sigma(a)\sigma(a)}^{\sigma^2(s)} \left(\varrho_{\sigma^2(s)}^{\sigma(a)\sigma(a)} \right)^t \chi_q(\sigma^2(s)) = \left(\varrho_{\sigma^2(0)}^{\sigma(0)\sigma(0)} \right)^t \left(\varrho_{\sigma(a)}^{\sigma(0)a} \right)^{2t} \sum_s N_{aa}^s \left(\varrho_s^{aa} \right)^t \chi_q(s), \quad (3.19)$$

upon insertion of an S -channel spectral decomposition on each side of eq. (3.18). Since $\sigma^2(0)$ always appears in $\sigma(0) \otimes \sigma(0)$ with multiplicity one we can use eq. (3.13) to find that

$$\eta_{\sigma^2(0)}^{\sigma(0)\sigma(0)} = (-1)^K, \quad (3.20)$$

so that (using eq. (3.7))

$$\varrho_{\sigma^2(0)}^{\sigma(0)\sigma(0)} \left(\varrho_{\sigma(a)}^{\sigma(0)a} \right)^2 = \exp[i\pi(N+1)l_{N-1}(a)] \exp\left[i\pi \frac{N+1}{N} (r(\sigma(a)) + r(a))\right]. \quad (3.21)$$

Using this result, eq. (3.19) becomes

$$\sum_s \chi_q(s) \left(e^{-i\pi h(s)} \right)^t N_{aa}^s \left\{ \eta_s^{aa} - \exp\left[-i\pi(r(a) + r(\sigma(a))) + \Delta_s^{aa} + \Delta_{\sigma(s)}^{a\sigma(a)} + (N+1)l_{N-1}(a)\right] \eta_{\sigma^2(s)}^{\sigma(a)\sigma(a)} \right\} = 0. \quad (3.22)$$

(Note that, unlike eq. (3.13), there is no factor of N multiplying either Δ .) Consider first the terms with single-multiplicity representations s . If N is odd these vanish identically (due to eq. (3.13)), while if N is even the expression in curly brackets reduces to

$$\eta_s^{aa} \{1 - \exp[i\pi l_{N-1}(s)]\}. \quad (3.23)$$

Now consider the terms where s occurs with multiplicity in the tensor product. It is important to realize that, although $N_{\sigma(a)\sigma(a)}^{\sigma^2(s)} = N_{aa}^s$ implies that (cf. eq. (A.19))

$$N_{\sigma(a)\sigma(a)}^{\sigma^2(s)} = N_{\sigma(a)\sigma(a)}^{+\sigma^2(s)} + N_{\sigma(a)\sigma(a)}^{-\sigma^2(s)} = N_{aa}^{+s} + N_{aa}^{-s} = N_{aa}^s,$$

the map σ has not been defined for symmetric versus anti-symmetric copies in an intermediate channel. We would like to define it so that the cases of multiplicities and no multiplicities agree. If eq. (3.22) is written with the multiplicities of symmetric and anti-symmetric terms explicitly displayed, it becomes an equation for the differences $\Delta N_{ab}^s = N_{ab}^{+s} - N_{ab}^{-s}$

$$\sum_s \chi_q(s) (e^{-\pi i h(s)})^t \left\{ \Delta N_{aa}^s - \exp[-i\pi(r(a) + r(\sigma(a)) + \Delta_s^{aa} + \Delta_{\sigma(s)}^{a\sigma(a)} + (N+1)l_{N-1}(a))] \Delta N_{\sigma(a)\sigma(a)}^{\sigma^2(s)} \right\} = 0. \quad (3.24)$$

If N is odd we can allow the sum to just run over the terms with tensor multiplicity greater than one, while if N is even we must include the single-multiplicity terms. Since this equation must hold for all integers t , it will hold only if both the expression in curly brackets in (3.23) vanishes (for N even) and if

$$N_{\sigma(a)\sigma(a)}^{+\sigma^2(s)} - N_{\sigma(a)\sigma(a)}^{-\sigma^2(s)} = \pm (N_{aa}^{+s} - N_{aa}^{-s})$$

(where the \pm sign is just that in eq. (3.24)). Then the map σ can be extended so that

$$\begin{aligned} \mathcal{Q}_{\sigma^2(s)}^{\sigma(a)\sigma(a)} &= \exp[i\pi(N+1)l_{N-1}(a)] \exp\left[i\pi \frac{N+1}{N} (r(\sigma(a)) + r(a))\right] \mathcal{Q}_s^{aa} \\ &= \exp\left[i\pi \frac{N+1}{N} K\right] \exp\left[2\pi i \frac{r(a)}{N}\right] \mathcal{Q}_s^{aa} \quad (\text{SU}(N), \text{ all } N) \end{aligned} \quad (3.25)$$

holds, even in the case of fusion multiplicities. While this agrees transparently with the direct calculation in the case of N odd (3.15), for N even it implies the

Proposition. s multiplicity free in $a \otimes a$ and $\sigma^2(s)$ multiplicity free in $\sigma(a) \otimes \sigma(a)$ imply that $l_{N-1}(s)$ and $l_{N-1}(\sigma^2(s))$ are even.

The interesting contrapositive,

With $s \in a \otimes a$ and $\sigma^2(s) \in \sigma(a) \otimes \sigma(a)$ in $SU(2n)$, if $l_{2n-1}(s)$ or $l_{2n-1}(\sigma^2(s))$ is odd, then either s occurs with multiplicity in $a \otimes a$, or $\sigma^2(s)$ occurs with multiplicity in $\sigma(a) \otimes \sigma(a)$,

is a useful (though incomplete) diagnostic for the presence of $SU(N)$ tensor ring multiplicities. For the remaining groups we obtain the relatively uncomplicated formulas

$$\eta_{\sigma^2(s)}^{\sigma(a)\sigma(a)} = \eta_s^{aa} \times \begin{cases} e^{i\pi NK} & \text{for } \text{Sp}(N) \\ 1 & \text{E}_6, \text{so}(2n+1), \text{ and } \sigma_1 \text{ of } \text{so}(4n) \\ (-1)^{nK} & \sigma_2 \text{ of } \text{so}(4n) \\ (-1)^K & \text{E}_7 \text{ and } \text{so}(4n+2). \end{cases} \quad (3.26)$$

in the multiplicity-free case. The orthogonal group results hold for a either a tensor or spinor. Examination of these values shows that

$$\eta_{\sigma^2(s)}^{\sigma(a)\sigma(a)} = \eta_s^{aa} (-1)^{(\kappa|\sigma(0))} \times \begin{cases} (-1)^{l_{2n}(s)} & \text{SU}(2n+1) \\ 1 & \text{otherwise} \end{cases} \quad (3.27)$$

is correct in all cases. Explicitly,

$$(\kappa|\sigma(0)) = K \times \begin{cases} 1 & \text{SU}(N) \\ 2 & \text{E}_6, \text{so}(2n+1), \text{so}(4n) \text{ if } \sigma = \sigma_1 \\ 3 & \text{E}_7 \\ 2n-1 & \text{so}(4n+2) \\ n & \text{so}(4n) \text{ if } \sigma = \sigma_2 \\ N & \text{Sp}(N). \end{cases} \quad (3.28)$$

The trefoil-type-knot-based argument then yields, with p the order of the automorphism σ ,

$$\mathcal{Q}_{\sigma^2(s)}^{\sigma(a)\sigma(a)} = e^{2\pi i q(a)} \exp \left[i\pi \frac{p+1}{p} (\kappa|\sigma(0)) \right] \mathcal{Q}_s^{aa}, \quad (3.29)$$

for all groups and all representations. It also implies that if s and $\sigma^2(s)$ are multiplicity free in $\text{so}(4n+2)$ Kronecker squares, then $l_1(s)$ and $l_1(\sigma^2(s))$ are even, and if multiplicity free in Kronecker squares of E_6 , then $a_2(s) + a_6(s)$ and $a_2(\sigma^2(s)) + a_6(\sigma^2(s))$ are even.

Only eqs. (3.1)–(3.6) will be needed for the arguments in the rest of this section. This means that the following arguments hold for *all* Chern–Simons theories that display simple-current symmetries. Eq. (3.29) will, however, be relevant for the results of sect. 6 that involve knot expectation values.

3.3. CO-MINIMAL EQUIVALENCE OF TETRAHEDRA

We will henceforth display compatible sets of S , T , and U fusion rule channels without the fusion coefficients written explicitly by assuming that the sums only run over the representations with non-zero coefficients (but with multiplicity). For example, the fusion rules in eq. (2.6) can be written compactly (with a slight abuse of notation) as

$$\begin{array}{lll} \text{S-channel} & \text{T-channel} & \text{U-channel} \\ a \cdot b = \sum_s s, & a \cdot \rho(c) = \sum_t t, & a \cdot \rho(d) = \sum_u u, \\ c \cdot d = \sum_s s, & \rho(b) \cdot d = \sum_t t, & \rho(b) \cdot c = \sum_u u. \end{array} \quad (3.30)$$

The associated matrices of expectation values of tetrahedra are real and satisfy non-linear equations that only depend on the coefficients appearing in eq. (2.26) (and on those in eq. (2.30) for link-type tetrahedra). We now consider the co-minimally equivalent set of fusion rules

$$\begin{array}{lll} \text{S-channel} & \text{T-channel} & \text{U-channel} \\ \sigma(a) \cdot b = \sum_s \sigma(s), & \sigma(a) \cdot \rho(c) = \sum_t \sigma(t), & \sigma(a) \cdot \rho(\sigma(d)) = \sum_u u, \\ c \cdot \sigma(d) = \sum_s \sigma(s), & \rho(b) \cdot \sigma(d) = \sum_t \sigma(t), & \rho(b) \cdot c = \sum_u u. \end{array} \quad (3.31)$$

The sums here run over the same representations that appear in eq. (3.30). The pairs of fusion rules displayed here exist due to eq. (3.1) (or the second equality in (3.7)) and due to the fact that

$$\rho(\sigma(a)) = \sigma^{-1}(\rho(a)). \quad (3.32)$$

Each channel provides a basis that spans a new Hilbert space \mathcal{H}_σ of the same dimensionality f as \mathcal{H} . The tetrahedral expectation values satisfy eqs. (2.25) and (2.26), but with the coefficients in (2.26) now given by

$$\mathcal{Q}_{\sigma(s)}^{c\sigma(d)} \mathcal{Q}_{\sigma(t)}^{\sigma(a)\rho(c)} \mathcal{Q}_u^{\rho(b)c} \mathcal{F}_c^{-1}. \quad (3.33)$$

Insertion of the identities in eq. (3.5) shows that the complex part of the relative phases cancels so that

$$\mathcal{Q}_{\sigma(s)}^{c\sigma(d)} \mathcal{Q}_{\sigma(t)}^{\sigma(a)\rho(c)} \mathcal{Q}_u^{\rho(b)c} \mathcal{F}_c^{-1} = \pm \mathcal{Q}_s^{cd} \mathcal{Q}_t^{a\rho(c)} \mathcal{Q}_u^{\rho(b)c} \mathcal{F}_c^{-1} \quad (3.34)$$

This means that the coefficients in the equations that determine the two sets of tetrahedra are equal up to sign, so that corresponding tetrahedra appearing in the two cases are equal up to sign. Pictorially, by going to the co-minimally-equivalent set of fusion rules we have changed the representations around a particular closed oriented loop uniformly by $r \rightarrow \sigma(r)$. The same result holds in general for all other loops and for iterations around each loop. In all cases the channels that appear

produce exactly the same set of constraining equations up to sign. The general result is that

$$\begin{array}{c} \sigma^{n+m-l}(c) \\ \nearrow \sigma^l(d) \\ \sigma^{n+m}(s) \quad \sigma^{l-m}(t) \\ \nwarrow \sigma^m(b) \\ \sigma^n(a) \end{array} = \pm \begin{array}{c} c \\ \nearrow d \\ s \quad t \\ \nwarrow b \\ a \end{array} \quad (3.35)$$

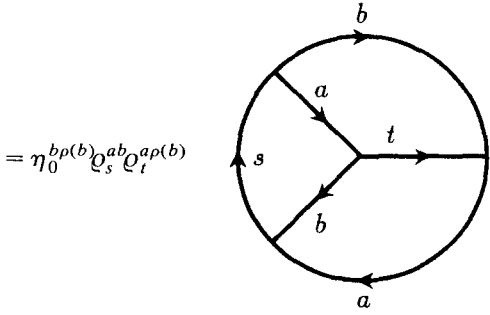
This is all that one can say about the general case of non-link-type tetrahedra, since the sign of each tetrahedron is a matter of residual vertex normalization. For link-type tetrahedra note that the coefficients in the equations in eq. 2.30 are squares and so do not depend on any of the undetermined signs in eq. 3.5. Therefore, using eq. 3.35, as well as eq. 3.5 in eq. 2.30, we obtain the exact result

$$\begin{array}{c} b \\ \nearrow \sigma(a) \\ \sigma(s) \quad \sigma(t) \\ \nwarrow b \\ \sigma(a) \end{array} = Q_s^{ab} Q_t^{ap(b)} \begin{array}{c} b \\ \nearrow a \\ s \quad t \\ \nwarrow b \\ a \end{array} \quad (3.36)$$

While the permutation sign $\eta_0^{b\rho(b)}$ cancels trivially in this particular case, the general result

$$\begin{array}{c} \sigma^m(b) \\ \nearrow \sigma^n(a) \\ \sigma^{n+m}(s) \quad \sigma^{n-m}(t) \\ \nwarrow \sigma^m(b) \\ \sigma^n(a) \end{array}$$

$\eta_0^{\sigma^m(b)\rho(\sigma^m(b))} Q_{\sigma^{n+m}(s)}^{\sigma^n(a)\sigma^m(b)} Q_{\sigma^{n-m}(t)}^{\sigma^n(a)\rho(\sigma^m(b))}$



(3.37)

contains contributions from these signs. The product of these charge conjugation signs is given by

$$\eta_0^{\sigma^m(b)\rho(\sigma^m(b))} \eta_0^{b\rho(b)} = (-1)^{m(p-1)(\kappa|\sigma(0))}. \quad (3.38)$$

The complex parts of all the phases in eqs. (3.36) and (3.37) cancel leaving only a calculable sign. This relative sign results both from the transformation property of the permutation signs and from that of the conformal dimensions involved. While one might hope that the permutation signs could be chosen in such a way that the signs of tetrahedra are uniform within cominimal equivalence classes, simple counter-examples exist in which it is impossible to arrange this, even using all possible freedoms of normalizations.

4. Rank-level duality of planar tetrahedra

The aim of this section is to show that each tetrahedron in an $SU(N)_K$, $Sp(N)_K$, or $so(2n+1)_{2k+1}$ theory has at least one partner in $SU(K)_N$, $Sp(K)_N$, or $so(2k+1)_{2n+1}$, respectively, with the same expectation value up to sign. In the case of $so(2n+1)_{2k+1}$ this only applies to tetrahedra with tensor representations on all edges. The results of sect. 3 then show that each tetrahedron is also dual to entire co-minimal equivalence classes of tetrahedra that all have the same expectation value (up to sign).

The map between integrable representations of $G(N)_K$ and its rank-level dual $G(K)_N$ given by tableau transposition

$$a \in G(N)_K \rightarrow \tilde{a} \in G(K)_N \quad (4.1)$$

connects representations with closely related quadratic Casimirs, fusion coeffi-

cients, and q -dimensions, as follows. In order to treat $SU(N)$, $Sp(N)$, and $so(2n+1)$ in parallel, we extend eq. (3.11) by defining

$$\Delta_c^{ab} = \begin{cases} (r(a) + r(b) - r(c))/N & SU(N) \\ r(a) + r(b) - r(c) & so(2n+1) \\ 0 & Sp(N). \end{cases} \quad (4.2)$$

For all three groups the non-zero fusion coefficients of $G(N)_K$ are related to those of $G(K)_N$ by [7,8]

$$N_{ab}^c = N_{\bar{a}\bar{b}}^{\sigma^{ab}(\bar{c})}. \quad (4.3)$$

(Note that the naïve relation $N_{ab}^c = N_{\bar{a}\bar{b}}^{\bar{c}}$ does *not* hold in general for the fusion coefficients.) For any tensor representation [3,13,24] a

$$h(a)_{G(N)_K} + h(\bar{a})_{G(K)_N} = \begin{cases} \frac{r(a)}{2} \left(1 - \frac{r(a)}{NK}\right) & \text{for } SU(N)_K \\ \frac{r(a)}{2} & \text{for } so(N)_K \text{ and } Sp(N)_K. \end{cases} \quad (4.4)$$

In addition [7], if $s \in a \otimes b$,

$$h(s)_{G(N)_K} + h(\sigma^{\Delta_s^{ab}}(\bar{s}))_{G(K)_N} = \begin{cases} \frac{r(a) + r(b)}{2} \left(1 - \frac{r(a) + r(b)}{NK}\right) + \Omega^{ab}(s) & \text{for } SU(N)_K \\ \frac{r(a) + r(b)}{2} - \Gamma^{ab}(s) & \text{for } so(2n+1)_{2k+1} \\ & \text{and } Sp(N)_K, \end{cases} \quad (4.5)$$

where $\Gamma^{ab}(s)$ denotes the number of contractions (of tensor indices) needed to obtain s in the tensor product $a \otimes b$ and

$$\Omega^{ab}(s) = \sum_{i=K-\Delta_s^{ab}+1}^K c_i(s). \quad (4.6)$$

where the $c_i(s)$ are the column lengths of the reduced tableau s . Both quantities are integers. In addition, the q -dimensions satisfy [3,12]

$$\{\chi_q(a)\}_{G(N)_K} = \{\chi_q(\bar{a})\}_{G(K)_N}. \quad (4.7)$$

Without considering the exact values of the permutation signs, these equations yield the braid eigenvalue relations

$$\varrho_s^{ab} \varrho_{\sigma \Delta_s^{ab}(\bar{s})}^{\bar{a}\bar{b}} = (\pm)_s e^{\pi i \Phi(a,b)}. \quad (4.8)$$

where the sign $(\pm)_s$ depends on the intermediate channel s in a complicated way. Here, and henceforth,

$$\Phi(a, b) = \begin{cases} r(a)r(b)/NK & \text{SU}(N)_K \\ 0 & \text{so}(N)_K \text{ and } \text{Sp}(N)_K. \end{cases} \quad (4.9)$$

The dual identities for the special tetrahedral quantity in eq. (2.31) will only require these identities.

For the case of (linked) knots it will also be important to understand how the permutation signs η_s^{aa} and $\eta_{\sigma \Delta_s^{aa}(\bar{s})}^{\bar{a}\bar{a}}$ are related. We find that

$$\eta_s^{aa} \eta_{\sigma \Delta_s^{aa}(\bar{s})}^{\bar{a}\bar{a}} = \begin{cases} e^{i\pi r(a)} e^{i\pi \Omega^{aa}(s)} & \text{for } \text{SU}(N)_K \\ e^{i\pi r(a)} e^{i\pi \Gamma^{aa}(s)} & \text{for } \text{Sp}(N)_K \text{ and } \text{so}(N)_K. \end{cases} \quad (4.10)$$

In the appendix we obtain a proof of (4.10) for $\text{Sp}(N)_K$, $\text{so}(2n+1)_{2k+1}$, and for $\text{SU}(N)_K$ in the special case $\Omega^{aa}(s) = 0$ (which often occurs for $\Delta_s^{aa} \neq 0$), if s does not appear with reduced multiplicity. While eq. (6.37) implies eq. (4.10) without any such restrictions via an argument using the t twisted trefoil-type knot analogous to that of sect. 3, we do not have an independent proof of eq. (6.37) unless $t = \pm 1$, the case of the twisted unknot [3],

$$\left\langle \begin{array}{c} \text{Diagram of a knot with label } a \end{array} \right\rangle_{G(N)_K} = e^{i\pi r(a)} e^{\pi i \Phi(a,a)} \left\langle \begin{array}{c} \text{Diagram of a knot with label } \bar{a} \end{array} \right\rangle_{G(K)_N} \quad (4.11)$$

Insertion of an S -channel spectral decomposition on both sides yields (by using eqs. (4.3)–(4.7))

$$\sum_s N_{aa}^s \chi_q(s) e^{-i\pi h(s)} \left[\eta_s^{aa} - e^{-i\pi(r(a) + \Omega^{aa}(s))} \eta_{\sigma \Delta_s^{aa}(\bar{s})}^{\bar{a}\bar{a}} \right] = 0, \quad (4.12)$$

which constitute two real equations for the difference between η_s^{aa} in $\text{SU}(N)_K$ and $\eta_{\sigma \Delta_s^{aa}(\bar{s})}^{\bar{a}\bar{a}}$ in $\text{SU}(K)_N$ (replace Ω with Γ for the other groups). If we use eq. (4.10) for the terms that appear with no reduced multiplicity (or with $\Omega^{aa}(s) = 0$ for $\text{SU}(N)$), then we obtain two equations for the cases with reduced multiplicity (or for those with $\Omega^{aa}(s) \neq 0$). This yields a proof of a restricted but infinite set of cases where eq. (4.10) holds for all s and with $\Omega^{aa}(s) \neq 0$ in the case of $\text{SU}(N)$. (That the map in eq. (4.1) is undefined between symmetric and anti-symmetric

copies of the same tableau in an intermediate channel gives one the freedom to define it so that eq. (4.10) will continue to hold in the case of multiplicity.)

While the product of permutation signs *does* depend on certain details of the intermediate channel, the product of braid eigenvalues does not:

$$\varrho_s^{aa} \varrho_{\sigma^{\Delta_{aa}^a}(\tilde{s})}^{\tilde{a}\tilde{a}} = e^{i\pi r(a)} e^{\pi i \Phi(a,a)}. \quad (4.13)$$

That the product does not depend on the intermediate channel is the result of a remarkable cancellation between the permutation signs and a contribution from the conformal dimensions.

4.1. TETRAHEDRAL DUALITY

Given the set of compatible fusion rule channels specified in eq. (3.30) in the level K $G(N)$ theory, we now consider a dual set of fusion rules in the level N $G(K)$ theory,

$$\begin{aligned} & \begin{array}{c} S\text{-channel} \\ \tilde{a} \cdot \tilde{b} = \sum_s \sigma^{\Delta_s^{ab}}(\tilde{s}), \end{array} & \begin{array}{c} T\text{-channel} \\ \tilde{a} \cdot \rho(\tilde{c}) = \sum_t \sigma^{\Delta_{ct}^a}(\tilde{t}), \end{array} & \begin{array}{c} U\text{-channel} \\ \tilde{a} \cdot \rho(\sigma^\delta(\tilde{d})) = \sum_u \sigma^{\Delta_{bu}^a}(\tilde{u}), \end{array} \\ & \tilde{c} \cdot \sigma^\delta(\tilde{d}) = \sum_s \sigma^{\Delta_s^{ab}}(\tilde{s}), & \rho(\tilde{b}) \cdot \sigma^\delta(\tilde{d}) = \sum_t \sigma^{\Delta_{ct}^a}(\tilde{t}), & \rho(\tilde{b}) \cdot \tilde{c} = \sum_u \sigma^{\Delta_{bu}^a}(\tilde{u}). \end{aligned} \quad (4.14)$$

The letters a, \dots, t, u denote $G(N)_K$ representations and the “tilde” symbol again denotes the map from $G(N)_K$ integrable representations to $G(K)_N$ integrable representations given by tableau transposition. In addition, for $\mathrm{Sp}(N)_K$ and $\mathrm{SO}(2n+1)_{2k+1}$, $\rho(a) = a$ for all representations a . The integer Δ_c^{ab} is defined in eq. (4.2) and the quantity

$$\delta \equiv \Delta_s^{ab} - \Delta_s^{cd} \quad (4.15)$$

measures the failure of exact conservation of the number of boxes across an intermediate (here the S -) channel. We have also adopted a generalization of the index convention implicit in Δ_c^{ab} : an upper (lower) index indicates that r comes in with a plus (minus) sign. For example,

$$\Delta_{bc}^a = \begin{cases} (r(a) - r(b) - r(c))/N & \text{for } \mathrm{SU}(N)_K \\ r(a) - r(b) - r(c) & \text{for } \mathrm{SO}(2n+1)_{2k+1} \\ 0 & \text{for } \mathrm{Sp}(N)_K. \end{cases} \quad (4.16)$$

In all cases in which they appear these will be integers; in the example just given this quantity would only appear for $c \in a \otimes \rho(b)$.

This dual set of fusion rules consistently defines three f -dimensional bases of a $G(K)_N$ Hilbert space, with each channel corresponding to a pair of compatible fusion rules. This follows from the dual and cominimal properties of the fusion coefficients in eqs. (4.3) and (3.7), respectively, as well as eq. (3.32). For $SU(N)_K$ the identity

$$\rho(\tilde{a}) = \sigma^{K-l_1(a)}(\widetilde{\rho(a)}) \quad (4.17)$$

is also needed. This last identity is readily demonstrated by implementing the operations on each side of the equation diagrammatically (i.e. via a series of Young tableaux). The existence of this dual set of fusion channels establishes a well-defined map from tetrahedra in one theory to those of the other.

Corresponding to these two sets of fusion rules is the following simple relation between the S - and T -channel products of braid matrix eigenvalues:

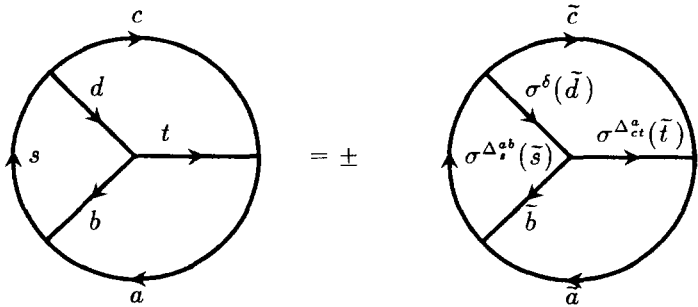
$$\begin{aligned} Q_s^{ab} Q_{\sigma^{\Delta_{\tilde{s}}^a}(\tilde{s})}^{\tilde{a}\tilde{b}} &= \pm e^{\pi i \Phi(a,b)}, \\ Q_t^{a\rho(c)} Q_{\sigma^{\Delta_{\tilde{t}}^a}(\tilde{t})}^{\tilde{a}\rho(\tilde{c})} &= \pm e^{-\pi i \Phi(a,c)}. \end{aligned} \quad (4.18)$$

(The analogous U -channel identities are obtained as cases of the T -channel identity by setting $c \rightarrow d$, etc.)

Using these equations and eq. (3.5) we find that the products of eigenvalues that appear as coefficients in the two sets of non-linear constraint equations corresponding to the two sets of fusion rules in (3.30) and (4.14) are the same up to sign for general tetrahedra

$$Q_s^{cd} Q_t^{a\rho(c)} Q_u^{\rho(b)c} \mathcal{F}_c^{-1} = \pm \mathcal{F}_{\tilde{c}} \left(Q_{\sigma^{\Delta_{\tilde{s}}^a}(\tilde{s})}^{\tilde{c}\sigma^{\tilde{b}}(\tilde{d})} Q_{\sigma^{\Delta_{\tilde{t}}^a}(\tilde{t})}^{\tilde{a}\rho(\tilde{c})} Q_{\sigma^{\Delta_{\tilde{u}}^a}(\tilde{u})}^{\rho(\tilde{b})\tilde{c}} \right)^{-1}. \quad (4.19)$$

Given this result it immediately follows from the nonlinear set of equations (eqs. (2.25) and (2.26)) that the tetrahedra of one theory and the dual tetrahedra of the dual theory satisfy exactly the same set of equations up to sign. The result for general tetrahedra is that



$$= \pm \quad (4.20)$$

For link-type tetrahedra (for which $\delta = 0$ always) the exact result

$$\begin{aligned}
 & \eta_0^{b\rho(b)} Q_s^{ab} Q_t^{a\rho(b)} \\
 & \quad \quad \quad \begin{array}{c} \text{Diagram 1: A circle with three internal lines meeting at a central vertex. The top-left line is labeled 'a' with an arrow pointing towards the center. The bottom-left line is labeled 'b' with an arrow pointing towards the center. The right line is labeled 't' with an arrow pointing away from the center. The top arc is labeled 'b' with an arrow pointing clockwise. The bottom arc is labeled 'a' with an arrow pointing clockwise. The left arc is labeled 's' with an arrow pointing counter-clockwise. } \end{array} \\
 & = \eta_0^{\tilde{b}\rho(\tilde{b})} \left(Q_{\sigma^{\Delta_s^{ab}}(\tilde{s})}^{\tilde{a}\tilde{b}} Q_{\sigma^{\Delta_{\tilde{t}}(\tilde{t})}}^{\tilde{a}\rho(\tilde{b})} \right)^{-1} \\
 & \quad \quad \quad \begin{array}{c} \text{Diagram 2: A circle with three internal lines meeting at a central vertex. The top-left line is labeled 'a' with an arrow pointing towards the center. The bottom-left line is labeled 'b' with an arrow pointing towards the center. The right line is labeled 't' with an arrow pointing away from the center. The top arc is labeled 'b' with an arrow pointing clockwise. The bottom arc is labeled 'a' with an arrow pointing clockwise. The left arc is labeled 's' with an arrow pointing counter-clockwise. } \end{array} \\
 & \hspace{15em} (4.21)
 \end{aligned}$$

follows from the supplemented skein relations (eqs. (2.26) and (2.30)), showing that the same product of tetrahedra and braid eigenvalues is an exact invariant under both types of discrete symmetries. The product of charge conjugation signs is given by

$$\eta_0^{b\rho(b)} \eta_0^{\tilde{b}\rho(\tilde{b})} = \begin{cases} (-1)^{(N+K)r(b)} & \text{for } \text{SU}(N)_K \\ 1 & \text{for } \text{Sp}(N)_K \text{ and } \text{so}(2n+1)_{2k+1}. \end{cases} \quad (4.22)$$

5. Two applications: WZW models and quantum groups

We give two simple applications of the above results.

5.1. WZW BRAID MATRICES

The WZW braid matrices are matrices of non-planar tetrahedra [1]. With the edge orientations in the definition of the WZW braid matrix in terms of Chern–

Simons graphs chosen to make the connection with the bases defined in subject. 2.1 transparent, consider the braid matrices specified by

$$\begin{array}{c} \begin{array}{c} b \quad b \\ \downarrow \quad \uparrow \\ a \rightarrow \quad \rightarrow s \quad \rightarrow \end{array} \end{array} a = \sum_t B_{st} \begin{bmatrix} b & \rho(b) \\ a & \rho(a) \end{bmatrix} \eta_0^{b\rho(b)} \begin{array}{c} \begin{array}{c} b \quad b \\ \swarrow \quad \searrow \\ a \rightarrow \quad \rightarrow t \quad \rightarrow \end{array} \end{array} a
 \quad (5.1)$$

which braid ϕ_b and $\phi_{\rho(b)}$ in the WZW correlation functions $\langle \phi_a \phi_b \phi_{\rho(b)} \phi_{\rho(a)} \rangle$. The relation to Chern–Simons tetrahedra is simply that

$$\begin{aligned}
 B_{st} \begin{bmatrix} b & \rho(b) \\ a & \rho(a) \end{bmatrix} &= \eta_0^{b\rho(b)} (\chi_q(a) \chi_q(b))^{-1} \quad \begin{array}{c} \begin{array}{c} t \\ \swarrow \quad \searrow \\ a \rightarrow \quad \rightarrow s \quad \rightarrow \end{array} \end{array} a \\
 &= (\chi_q(a) \chi_q(b))^{-1} \mathcal{F}_b^{-1} \eta_0^{b\rho(b)} \varrho_s^{ab} \varrho_t^{a\rho(b)} \quad \begin{array}{c} \begin{array}{c} b \\ \swarrow \quad \searrow \\ a \rightarrow \quad \rightarrow s \quad \rightarrow \end{array} \end{array} a
 \end{aligned}
 \quad (5.2)$$

This shows that the WZW braid matrices singled out by eq. (5.1) are expressible in terms of link-type tetrahedra. Since the planar tetrahedra appearing in eq. (5.2) are exactly those of F_{st} (with $d = a$ and $c = b$)

$$B_{st} \begin{bmatrix} b & \rho(b) \\ a & \rho(a) \end{bmatrix} = \mathcal{F}_b^{-1} (\eta_0^{b\rho(b)} \varrho_s^{ab} \varrho_t^{a\rho(b)} F_{st}). \quad (5.3)$$

Using this correspondence and eq. (4.21) we find that

$$\sum_t B_{s't} \begin{bmatrix} b & \rho(b) \\ a & \rho(a) \end{bmatrix} B_{\sigma^{-\Delta_{\bar{s}}^a(\bar{s})}\sigma^{-\Delta_{b\bar{t}}^a(\bar{t})}} \begin{bmatrix} \tilde{b} & \rho(\tilde{b}) \\ \tilde{a} & \rho(\tilde{a}) \end{bmatrix} = e^{-2\pi i(h(b)+h(\tilde{b}))} Q_{s'}^{ab} (Q_s^{ab})^{-1} \sum_t F_{s't} F_{st} \\ = e^{\pi i r(b)} e^{\pi i \Phi(b,b)} \delta_{s's}, \quad (5.4)$$

where $\Phi(b, b)$ is defined in eq. (4.9). This complements the results in refs. [3,24] on WZW braid- and fusion-matrix dualities. There, however, WZW braid matrices that braid the pair of ϕ_b fields in $\langle \phi_a \phi_b \phi_b \phi_d \rangle$ were considered. These latter braid matrices are proportional to a special class of non-link-type tetrahedra.

Similarly, the relation between the (link-type) WZW braid matrices that differ by co-minimal equivalence is found from eq. (3.36) to be

$$B_{\sigma(s)\sigma(t)} \begin{bmatrix} b & \rho(b) \\ \sigma(a) & \rho(\sigma(a)) \end{bmatrix} = B_{st} \begin{bmatrix} b & \rho(b) \\ a & \rho(a) \end{bmatrix}. \quad (5.5)$$

5.2. QUANTUM GROUP $6j$ -SYMBOLS AND WZW FUSION MATRICES

Given appropriate normalizations, the expectation values of planar tetrahedra equal [1] the values of quantum $6j$ -symbols (of $\mathcal{U}_q(G(N))$) evaluated at the roots of unity $q = \exp(2\pi i/(K + \bar{g}))$. (In addition, the WZW fusion matrices are also directly matrices of planar tetrahedra.) Therefore sect. 3 and 4 immediately yield identities for these quantities. Given the standard relation [25,26]

the correspondence is

The results of sect. 3 yield the transformation properties of quantum $6j$ -symbols

under co-minimal equivalence. For example,

$$\left\{ \begin{matrix} \sigma(a) & b & \sigma(s) \\ \sigma(c) & d & \sigma(u) \end{matrix} \right\}_q = \pm \left\{ \begin{matrix} a & b & s \\ c & d & u \end{matrix} \right\}_q. \quad (5.8)$$

Similarly, the results of sect. 4 show that there is a rank-level duality between the quantum $6j$ -symbols of $\mathcal{Z}_q(G(N))$ and $\mathcal{Z}_q(G(K))$ for q the common root of unity $q = \exp(2\pi i/(K + \bar{g}))$.

$$\left\{ \begin{matrix} a & b & s \\ c & d & u \end{matrix} \right\}_q = \pm \left\{ \begin{matrix} \tilde{a} & \tilde{b} & \sigma^{\Delta_{\tilde{s}}^{ab}}(\tilde{s}) \\ \tilde{c} & \tilde{d} & \sigma^{\Delta_{\tilde{u}}^{cd}}(\tilde{u}) \end{matrix} \right\}_q. \quad (5.9)$$

The \pm signs appearing in these two equations depend on the phase conventions of the $6j$ -symbols (which are inherited from the residual vertex normalization conventions of the planar tetrahedra via eq. (5.7)). Exact identities can also be constructed in the special case corresponding to link-type tetrahedra.

6. Discrete symmetries for all Chern–Simons observables

Arbitrary planar graphs can be reduced to sums of products of planar tetrahedra [14]. The overall sign of a non-link-type graph depends on the arbitrary normalizations of the graph vertices, and the tetrahedra that appear in its reduction can all have expectation values with normalization dependent signs. However, if we fix the normalization of all vertices of the original graph, then, since the new vertices that appear in the reduction process come in pairs, the pattern of relative signs between terms in the sum is *not* normalization dependent. It is not clear what determines these relative signs or how to calculate them. The situation does not change for link-type graphs. Such a graph has an unknown, intrinsic overall sign (since each vertex appears an even number of times in the graph, so that a change of normalization does not change the sign of the graph), and, in addition, the relative signs between terms in a tetrahedral decomposition are not known. Without a way of calculating these signs the algorithm in ref. [14] is ineffective for general graphs.

To make this problem concrete consider the graph

$G(a, b, \{s_i\}) =$

(6.1)

which has the reduction into generic tetrahedra

$$G(a, b, \{s_i\}) = \eta_0^{ap(a)} \eta_0^{bp(b)} (\chi_q(a) \chi_q(b))^{-1} (\chi_q(s_1) \chi_q(s_2) \chi_q(s_3) \chi_q(s_4))^{-1/2}$$

$$\sum_{t,ijkl} \frac{1}{\chi_q(t)} \times$$

$$(6.2)$$

The vertices not in common between each term in the sum (i.e., those that do not appear in the original graph) come in dual pairs so that a change of residual vertex normalization does not change the relative sign of the terms. Since this is a link-type graph the vertices of the original graph also appear in dual pairs so that its overall sign is also clearly normalization independent. While the non-linear identities (2.25), (2.26) do establish relations between the signs of certain tetrahedra, the tetrahedra that appear here are not in the same set of basis change coefficients and so are not related in this way.

Using the fusion rule identity in (3.7) one can show that to an arbitrary graph in a level K $G(N)$ theory there corresponds a class of topologically identical graphs obtained by uniformly replacing the representations along oriented, closed loops by cominimal equivalents. Similarly, using eq. (4.3), one can also show that in the level N $G(K)$ theory there are dual graphs with co-minimal equivalents of transposes of the $G(N)_K$ representations along the edges. In this latter case, however, the fusion rule identities only establish that to each vertex of one graph there is a dual vertex and one might ask whether these can be pieced together consistently. This is always possible since the integers δ (defined in eq. (4.15)), which measure the absence of exact box conservation across intermediate channels, sum to zero around closed loops. Then using the same pattern of reduction to

tetrahedra for both graphs and the symmetry results for these tetrahedra, we see that co-minimally equivalent graphs are identical functions of cominimally equivalent tetrahedra, and that dual graphs are identical functions of dual tetrahedra. However, we only know that the absolute values of these (real) tetrahedra are the same. Therefore the above sign ambiguity only allows one to conjecture that the results of sects. 3 and 4 generalize to arbitrary graphs.

The first part of this section is devoted to examining some exceptional cases of graphs which *can* be calculated by the above algorithm, providing further evidence for the above conjecture. We then find linear equations for any link-type graph. These play the same role for general graphs that the analogous linear equations did for tetrahedra. In the last part of this section a graph-independent argument yields the exact transformation property of knots and links under co-minimal equivalence. An immediate consequence is a demonstration of the transformation property of link-type graphs under co-minimal equivalence. We obtain (but do not prove) the analogous transformation identities for graphs, knots, and links under rank-level duality.

6.1. CALCULABLE LINK-TYPE GRAPHS

The graph in eq. (6.1) has the alternate reduction entirely in terms of link-type tetrahedra

$$\begin{aligned} G(a, b, \{s_i\}) &= (\chi_q(a)\chi_q(b))^2 \varrho_{s_1}^{ab} \varrho_{s_4}^{ab} (\varrho_{s_2}^{ab} \varrho_{s_3}^{ab})^{-1} \\ &\times \sum_t \chi_q(t)^{-1} (\eta_0^{b\rho(b)} \varrho_{s_1}^{ab} F_{s_1 t} \varrho_t^{a\rho(b)})^* (\eta_0^{b\rho(b)} \varrho_{s_2}^{ab} F_{s_2 t} \varrho_t^{a\rho(b)}) \\ &\times (\eta_0^{b\rho(b)} \varrho_{s_3}^{ab} F_{s_3 t} \varrho_t^{a\rho(b)}) (\eta_0^{b\rho(b)} \varrho_{s_4}^{ab} F_{s_4 t} \varrho_t^{a\rho(b)})^*, \end{aligned} \quad (6.3)$$

where $F_{s,t}$ is exactly that displayed in eq. (2.23) with $c = b$ and $d = a$. The braid eigenvalues all come from insertions of factors of unity in the form of products of braid eigenvalues, such as $\varrho_t^{a\rho(b)} (\varrho_s^{a\rho(b)})^*$. In this case the strategy outlined above is successful, and eq. (3.36) leads to

$$(\varrho_{\sigma(s_1)}^{\sigma(a)b} \varrho_{\sigma(s_4)}^{\sigma(a)b})^{-1} \varrho_{\sigma(s_2)}^{\sigma(a)b} \varrho_{\sigma(s_3)}^{\sigma(a)b} G(\sigma(a), b, \{\sigma(s_i)\}) = (\varrho_{s_1}^{ab} \varrho_{s_4}^{ab})^{-1} \varrho_{s_2}^{ab} \varrho_{s_3}^{ab} G(a, b, \{s_i\}). \quad (6.4)$$

Similarly, eq. (4.21) yields

$$\begin{aligned} &(\varrho_{s_1}^{ab} \varrho_{s_4}^{ab})^{-1} \varrho_{s_2}^{ab} \varrho_{s_3}^{ab} G(a, b, \{s_i\}) \\ &= \varrho_{\sigma^{\Delta_{s_1}^{ab}}(\tilde{s}_1)}^{\tilde{a}\tilde{b}} \varrho_{\sigma^{\Delta_{s_4}^{ab}}(\tilde{s}_4)}^{\tilde{a}\tilde{b}} \left(\varrho_{\sigma^{\Delta_{s_2}^{ab}}(\tilde{s}_2)}^{\tilde{a}\tilde{b}} \varrho_{\sigma^{\Delta_{s_3}^{ab}}(\tilde{s}_3)}^{\tilde{a}\tilde{b}} \right)^{-1} G(\tilde{a}, \tilde{b}, \{\sigma^{\Delta_{s_i}^{ab}}(\tilde{s}_i)\}). \end{aligned} \quad (6.5)$$

The entire complex part of the (combined) phase from both sides of each of these equations cancels, yielding the result that the related graphs have the same expectation values up to a (calculable) sign. Although other examples of graphs with such reductions can be found, it does not seem possible in general to reduce general link-type graphs into sums of products of *link-type* tetrahedra.

A general link-type graph can have several types of intermediate channel edges which differ from those occurring in eq. (6.1). In all, there are four types of such channels. Depending on the orientations of the edges adjacent to an intermediate channel edge, one can have an *S*- or *T*-channel. In addition, depending on whether the pair of representations adjacent to one vertex are permuted at the opposite vertex, one can have a *twist* (with permutation) or *parallel* (without permutation) edge. The four intermediate channel edges in eq. (6.1) are *S*-channel twist edges. Link-type tetrahedra exhibit both *S*-channel and *T*-channel twist edges, but parallel edges are not possible. A simple example with parallel edges is the graph

$$G(a, b, \{s_1, s_2, t\}) = \text{Diagram} \quad (6.6)$$

The reduction of this graph to tetrahedra

$$G(a, b, \{s_1, s_2, t\}) = \frac{\eta_0^{a\rho(a)}}{\sqrt{\chi_q(a)\chi_q(b)\chi_q(t)}} \times \sum_i \text{Diagram 1} \times \text{Diagram 2} \quad (6.7)$$

can be written in the form

$$\begin{aligned} & \eta_0^{a\rho(a)} \varrho_{s_1}^{ab} (\varrho_{s_2}^{ab})^{-1} G(a, b, \{s_1, s_2, t\}) \\ &= (\chi_q(a)\chi_q(b))^{3/2} \chi_q(t)^{-1/2} \\ & \times \sum_i \left(\eta_0^{b\rho(b)} \varrho_{s_1}^{ab} F_{s_1 t}(i) \varrho_t^{a\rho(b)} \right) \left(\eta_0^{b\rho(b)} \varrho_{s_2}^{ab} F_{s_2 t}(i) \varrho_t^{a\rho(b)} \right)^* , \end{aligned} \quad (6.8)$$

where the sum is over the $N_{a\rho(b)}^t$ types of the coupling \mathcal{K}_{bt}^a (or its dual) appearing at the indicated vertices. This example isolates a further problem, if the fusion multiplicity is greater than two. If the multiplicity is exactly two, then the two couplings (generally) correspond to symmetric and anti-symmetric combinations and the corresponding braid eigenvalues differ by a sign so that no degeneracy need occur. If, however, $N_{a\rho(b)}^t \geq 3$ for some t , a degeneracy will necessarily occur, in the sense that the braid eigenvalues occur with multiplicity. To apply the results of sects. 3 and 4 to this case (as well, in fact, to the previous case) we are implicitly assuming that an orthogonal basis of the degenerate couplings can be chosen so that the tetrahedra that only differ by such couplings are exactly equal. In the case of low multiplicity or where this is possible, we find that

$$\begin{aligned} & \eta_0^{\sigma(a)\rho(\sigma(a))} \varrho_{\sigma(s_1)}^{\sigma(a)b} \left(\varrho_{\sigma(s_2)}^{\sigma(a)b} \right)^{-1} G(\sigma(a), b, \{\sigma(s_1), \sigma(s_2), \sigma(t)\}) \\ &= \eta_0^{a\rho(a)} \varrho_{s_1}^{ab} \left(\varrho_{s_2}^{ab} \right)^{-1} G(a, b, \{s_1, s_2, t\}). \end{aligned} \quad (6.9)$$

In addition,

$$\begin{aligned} & \eta_0^{a\rho(a)} \varrho_{s_1}^{ab} \left(\varrho_{s_2}^{ab} \right)^{-1} G(a, b, \{s_1, s_2, t\}) \\ &= \eta_0^{\tilde{a}\rho(\tilde{a})} \left(\varrho_{\sigma^{\Delta_{s_1}^a}(\tilde{s}_1)}^{\tilde{a}\tilde{b}} \right)^{-1} \varrho_{\sigma^{\Delta_{s_2}^a}(\tilde{s}_2)}^{\tilde{a}\tilde{b}} G(\tilde{a}, \tilde{b}, \{\sigma^{\Delta_{s_1}^a}(\tilde{s}_1), \sigma^{\Delta_{s_2}^a}(\tilde{s}_2), \sigma^{\Delta_{bt}^a}(\tilde{t})\}) \end{aligned} \quad (6.10)$$

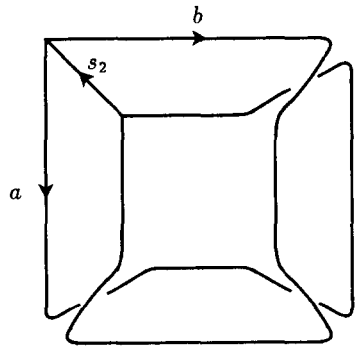
This example shows that no braid eigenvalue pre-factor appears for the parallel T -channel. (The same result holds for a parallel S -channel.)

6.2. LINEAR SKEIN RELATIONS FOR LINK-TYPE GRAPHS

Let us suppose that we have (presumably non-linear) equations that constrain the expectation values of a set of general graphs of a given topology. Then they should involve exactly the same sign ambiguity as the non-linear equations for tetrahedra. Therefore, for the graphs of this topology with edge representations and orientations chosen so that the graphs can support knots or links, their overall signs will be intrinsic but undetermined by these equations. The number of undetermined signs in the array of graphs $G(s_1, s_2, \dots; t_3, \dots)$, indexed by the intermediate channels, is $\sum_i f_i$. Here the sum is over the edges labeled as intermediate channels (in the case of graphs that support two-component links, this is just $(\# \text{ crossings}) \times f$). We now show how to construct (at least) this number of inhomogeneous linear equations. For each intermediate channel edge there will be two representations a and b at each vertex. From one vertex, trace out a Wilson line for a so that it follows the graph edges and eventually comes back to the other vertex of the intermediate channel edge. Then do the same for the representation

b , but in such a way that whenever a strand of a must be crossed, the b Wilson line goes uniformly over (or under) the a Wilson line. If there remain other external edges (bearing representations a_m) not traversed by this procedure trace out unlinked unknots until all edges have been traversed. The indicated (two-vertex) graph is just a fancy way of specifying a baryon (multiplied by a braid eigenvalue and, perhaps, a product of unknot expectation values) *. On the other hand at every crossing we can insert an S - or T -channel spectral decomposition and obtain the baryon as a sum of graphs from the array $G(s_1, s_2, \dots; t_3, \dots)$ (all of the same topology and with the same representations on the external legs).

For example, using the graph in eq. (6.1), we can draw


(6.11)

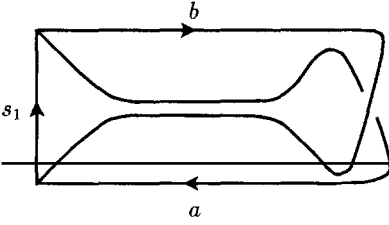
This graph leads to the equations

$$\begin{aligned}
 & (\varrho_{s_2}^{ab})^2 \sqrt{\chi_q(s_2)} (\chi_q(a) \chi_q(b))^2 \\
 &= \sum_{s_1, s_3, s_4} \sqrt{\chi_q(s_1) \chi_q(s_3) \chi_q(s_4)} (\varrho_{s_1}^{ab})^2 \left[(\varrho_{s_1}^{ab} \varrho_{s_4}^{ab})^{-1} \varrho_{s_2}^{ab} \varrho_{s_3}^{ab} G(a, b, \{s_1, s_2, s_3, s_4\}) \right]
 \end{aligned}
 \tag{6.12}$$

They have been written in a way that isolates (in square brackets) a special product of braid eigenvalues with the graph; it is exactly the special quantity in eqs. (6.4) and (6.5). These equations, with the unknowns considered to be the special products, are exact invariants of both co-minimal equivalence and rank-level duality, since the coefficients are squares of eigenvalues. This equation is a precise analog of the linear equations (2.30) found for link-type tetrahedra. In addition, other patterns of crossings lead to further equations. For example, the mirror image of the graph in (6.11) yields the complex conjugate of eq. 6.12.

* Actually, one can let the a strand cross the b strand in any way that leaves the graph topologically equivalent to a baryon; in which case further equations result.

Similarly, using the graph in eq. 6.6, we find that the non-planar graph


(6.13)

leads to the equation

$$\begin{aligned} & \sqrt{\chi_q(s_1)} (\chi_q(a) \chi_q(b))^{3/2} \\ &= \sum_{t, s_2} \sqrt{\chi_q(t) \chi_q(s_2)} \left[\eta_0^{a\rho(a)} \varrho_{s_1}^{ab} (\varrho_{s_2}^{ab})^{-1} G(a, b, \{s_1, s_2, t\}) \right] \end{aligned} \quad (6.14)$$

This equation has been written in a way that isolates the exact invariant of the discrete symmetries that appears in eqs. (6.9) and (6.10).

For arbitrary graphs the result is a set of equations, only slightly different for each of the four types of intermediate channels appearing in the graph. For each pair of representations a and b which join at (at least) one vertex in the graph, a subset of the following equations holds. Letting \mathcal{E} denote the number of intermediate edges of G , and \mathcal{W} the sum of the crossing signs of the (two-vertex) graph constructed above, the S -channel twist, T -channel twist, and parallel equations are

$$\begin{aligned} & \left(\prod_m \chi_q(a_m) \right) (\varrho_{s_l}^{ab})^{-\mathcal{W}} \sqrt{\chi_q(s_l)} \\ &= (\chi_q(a) \chi_q(b))^{-\mathcal{E}/2} \zeta \sum_{\{r_i, t_j, s_k (k \neq l)\}} \left(\prod_{i, j, k \neq l} \sqrt{\chi_q(r_i) \chi_q(t_j) \chi_q(s_k)} (\varrho_{t_j})^{w(j)} (\varrho_{s_k})^{-w(k)} \right) \\ & \quad \times G(a, b, \dots, \{r_i, t_j, s_k, \dots\}), \\ & \left(\prod_m \chi_q(a_m) \right) (\varrho_{t_l}^{a\rho(b)})^{\mathcal{W}} \sqrt{\chi_q(t_l)} \\ &= (\chi_q(a) \chi_q(b))^{-\mathcal{E}/2} \zeta \sum_{\{r_i, t_j (j \neq l), s_k\}} \left(\prod_{i, j \neq l, k} \sqrt{\chi_q(r_i) \chi_q(t_j) \chi_q(s_k)} (\varrho_{t_j})^{w(j)} (\varrho_{s_k})^{-w(k)} \right) \\ & \quad \times G(a, b, \dots, \{r_i, t_j, s_k, \dots\}), \end{aligned}$$

$$\begin{aligned}
& \left(\prod_m \chi_q(a_m) \right) \sqrt{\chi_q(t_l)} \\
&= (\chi_q(a) \chi_q(b))^{-\mathcal{C}/2} \zeta \sum_{\{r_i, t_j, s_k\}} \left(\prod_{i \neq l, j, k} \sqrt{\chi_q(r_i) \chi_q(t_j) \chi_q(s_k)} (\varrho_{t_j})^{w(j)} (\varrho_{s_k})^{-w(k)} \right) \\
&\quad \times G(a, b, \dots, \{r_i, t_j, s_k, \dots\}). \tag{6.15}
\end{aligned}$$

where, in each case, the index i labels parallel channels (either S - or T -type), the index j labels twist T -channels, and the index k labels twist S -channels. The representations a_m correspond to paths on the graph that yield unknots. In the third equation the crossing signs $w(j) = \pm 1$ for T -channel crossings and $w(k) = \pm 1$ for S -channel crossings satisfy the constraint that $\mathcal{W} = \sum_j w(j) + \sum_k w(k) = 0$. (The above construction implies that $\mathcal{W} = \pm 1$ in the first and second equations.) The omitted superscripts on the braid eigenvalues come from one of the pairs $\{a_m, a\}$, $\{a_m, b\}$, $\{a_{m_1}, a_{m_2}\}$, $\{a, b\}$ according to the edges adjacent to the intermediate channel in question. The sign ζ is given by

$$\zeta = \left(\prod_S \eta_0^{a\rho(a)} \eta_0^{b\rho(b)} \right) \left(\prod_T \eta_0^{a\rho(a)} \right), \tag{6.16}$$

where the products are over all S - and T -channel intermediate edges, respectively, and a and b are the adjacent edge representations of the given intermediate channel.

These equations provide as many constraints (with the complex conjugates twice as many) as undetermined signs for the family of graphs indexed by the representations appearing on the intermediate edges. Since we have, with the index i running over all intermediate edges, $\prod_i f_i$ graphs (for example, $f^{(\#\text{crossings})}$ graphs, for graphs supporting two-component links), these linear relations are insufficient in general to determine the graph expectation values.

They have, nevertheless, the same structure as the analogous equations for tetrahedra in eq. (2.30) and can be written in a similar manner to isolate a quantity that just depends on the squares of eigenvalues and on products of q -dimensions. If $f = 2$, they give a complete set of equations for the graphs in (6.1) and (6.6) and permit verification of the identities in eqs. (6.4), (6.5), (6.9) and (6.10) without appeal to any results about tetrahedra. This direct, linear approach to these identities does not require, in the case of fusion multiplicities, the existence of a special choice of basis for which tetrahedra of degenerate channels are equal. (Of course this problem recurs for the graphs themselves.)

In conclusion, it seems reasonably certain that

$$\begin{aligned} & \left(\prod_{k,j} \left(\varrho_{\sigma(s_k)}^{\sigma(a)b} \right)^{-w(k)} \left(\varrho_{\sigma(t_j)}^{\sigma(a)\rho(b)} \right)^{w(j)} \right) \zeta^\sigma G\left(\sigma(a), b, \dots, \{\sigma(r_i), \sigma(t_j), \sigma(s_k), \dots\}\right) \\ &= \left(\prod_{j,k} \left(\varrho_{s_k}^{ab} \right)^{-w(k)} \left(\varrho_{t_j}^{a\rho(b)} \right)^{w(j)} \right) \zeta G(a, b, \dots, \{r_i, t_j, s_k, \dots\}) \end{aligned} \quad (6.17)$$

for any choice of the signs $w(j)$ and $w(k)$ as long as $\sum_j w(j) + \sum_k w(k) = 0$, since these quantities satisfy some form of the relevant equations in (6.15) which are exactly invariant under co-minimal equivalence. The signs ζ and ζ^σ ($\tilde{\zeta}$ below) are defined by eq. (6.16), interpreted with reference to appropriate graphs.

Similarly, one expects

$$\begin{aligned} & \left(\prod_{j,k} \left(\varrho_{s_k}^{ab} \right)^{-w(k)} \left(\varrho_{t_j}^{a\rho(b)} \right)^{w(j)} \right) \zeta G(a, b, \dots, \{r_i, t_j, s_k, \dots\}) \\ &= \left(\prod_{j,k} \left(\varrho_{\sigma^{-1} s_k}^{\tilde{a}\tilde{b}} \right)^{w(k)} \left(\varrho_{\sigma^{-1} t_j}^{\tilde{a}\rho(\tilde{b})} \right)^{-w(j)} \right) \\ & \quad \times \tilde{\zeta} G(\tilde{a}, \tilde{b}, \dots, \{\sigma^{-1} r_i, \sigma^{-1} t_j, \sigma^{-1} s_k, \dots\}) \end{aligned} \quad (6.18)$$

to hold under the same condition on $w(j)$ and $w(k)$.

We have shown that eqs. (6.17) and (6.18) actually do hold for various particular graphs. In addition, the linear constraints that exist for any link-type graph also support the expectation that these equations will hold for all link-type graphs.

6.3. SYMMETRIES FOR LINKS AND KNOTS

Using eq. (3.5) we find that the characteristic polynomial of the square of the braid matrix $B_{\sigma(a)b}$

$$\prod_s \left(B_{\sigma(a)b}^2 - \left(\varrho_{\sigma(s)}^{\sigma(a)b} \right)^2 \right) = 0 \quad (6.19)$$

transforms to

$$\prod_s \left(\left(e^{-\pi i q(b)} B_{\sigma(a)b} \right)^2 - \left(\varrho_s^{ab} \right)^2 \right) = 0, \quad (6.20)$$

which is exactly the characteristic equation for the square of the braid matrix B_{ab} ,

$$\prod_s \left(B_{ab}^2 - \left(\varrho_s^{ab} \right)^2 \right) = 0. \quad (6.21)$$

This implies that a link $\mathcal{L}(\sigma(a), b, \dots)$ with $\sigma(a)$ on an unknotted component and the same link with a replacing $\sigma(a)$, $\mathcal{L}(a, b, \dots)$, multiplied by a phase $\exp(\pm i\pi q(b))$ for each (\mp signed) crossing for each component that the a component crosses, satisfy identical skein relations. Similarly, using eq. (4.8) the characteristic polynomial of the square of the $G(N)_K$ braid matrix B_{ab} can be written (with $\Phi(a, b)$ defined in eq. (4.9))

$$\prod_s \left(\left(e^{-\pi i \Phi(a, b)} B_{ab} \right)^2 - \left(Q_{\sigma^{-1} \Delta_{\mathbb{Z}}^b(s)}^{\bar{a}\bar{b}} \right)^{-2} \right) = 0, \quad (6.22)$$

which is exactly the characteristic equation for the square of the braid matrix $B_{\bar{a}\bar{b}}^{-1}$ in the $G(K)_N$ theory. This implies that a linking of unknots $\mathcal{L}(a, b, \dots)$ in a $G(N)_K$ theory will satisfy the same skein relation as the mirror image link in the $G(K)_N$ theory multiplied by a phase $e^{\pm \pi i \Phi(a, b)}$ for each (\pm signed) crossing of components a and b (and this holds for each pair of components). Similar statements result from comparison of the characteristic polynomial of the knot-type braid matrix $B_{\sigma(a)\sigma(a)}$

$$\prod_s \left(B_{\sigma(a)\sigma(a)} - Q_{\sigma^2(s)}^{\sigma(a)\sigma(a)} \right) = 0 \quad (6.23)$$

with that of B_{aa} (by using eq. (3.29) which relates the braid eigenvalues). A comparison of the characteristic polynomial for B_{aa} in a $G(N)_K$ theory with that for $B_{\bar{a}\bar{a}}$ in a $G(K)_N$ theory requires the use of eq. 4.13 (which we have proved in many but not all cases). Since not all knots or links can be untied with the skein relations corresponding to characteristic polynomials (such as (6.21) or (6.23)), these results alone would only permit the comparison of a restricted class of knots and links.

In the case of the Dynkin diagram symmetries a cabling argument yields a proof of the exact connection between any link and its cominimal equivalents (eq. (6.30) below). To obtain the analogous rank-level link relation (eq. (6.37)) we will need to examine the case of general knots and links by means of the reduction to planar graphs followed by an appeal to eq. (6.18). This will provide a complete proof of eq. (6.37) only for special classes of links (i.e. those built on certain special graphs such as those studied in subsects. 6.1 and 6.2).

Consider an arbitrary link $\mathcal{L}(\{a_i\})$ with representations a_i on the link components and the cominimally equivalent link $\mathcal{L}(\sigma(a_i), \{a_j, j \neq i\})$. The exact relation between these links is obtained as follows. Given any link \mathcal{L} , with a specified component \mathcal{K} , let $\{\mathcal{L}_s, \phi_s \in \phi_a \cdot \phi_b\}$ be the set of links with representations s on that component, and let $\mathcal{K}_a \cdot \mathcal{L}_b$ be the link with an untwisted, two-cable of the component \mathcal{K} in place of the original component. Then

$$\langle \mathcal{K}_a \cdot \mathcal{L}_b \rangle = \sum_s \langle \mathcal{L}_s \rangle, \quad (6.24)$$

always holds. This fact and the fusion rule for cominimal representations, $\phi_{\sigma(0)} \cdot \phi_a = \phi_{\sigma(a)}$, permits replacement of the Wilson line with $\sigma(a_i)$ with the two-cable of Wilson lines with a_i and $\sigma(0)$ on the two (everywhere locally parallel) lines, in order to obtain

$$\langle \mathcal{L}(\sigma(a_i), \{a_j, j \neq i\}) \rangle = \langle \mathcal{H}_{\sigma(0)} \cdot \mathcal{L}(\{a_i\}) \rangle. \quad (6.25)$$

Then the one-term skein relation based on the characteristic polynomial (of the same fusion rule)

$$B_{\sigma(0)r} = \left(\varrho_{\sigma(r)}^{\sigma(0)r} \right)^2 B_{\sigma(0)r}^{-1} = e^{2\pi i q(r)} B_{\sigma(0)r}^{-1}, \quad (6.26)$$

for $r = a, b, \dots$, can be used to lift up the $\sigma(0)$ component, $\mathcal{H}_{\sigma(0)}$, detaching it from the rest of the link, at the cost of one factor of the braid eigenvalue in eq. 6.26 (or its inverse) for every negative (positive) *under-crossing* by $\mathcal{H}_{\sigma(0)}$ of any other component, to obtain

$$\begin{aligned} & \langle \mathcal{L}(\sigma(a_i), \{a_j, j \neq i\}) \rangle \\ &= \exp(-i\pi \sum_{j \neq i} q(a_j) w(i, j)) \exp(-2\pi i q(a_i) w(i, i)) \langle \mathcal{H}_{\sigma(0)} \rangle \langle \mathcal{L}(\{a_i\}) \rangle. \end{aligned} \quad (6.27)$$

where $w(i, j)$ is the sum of the crossing signs [18] between the components i and j . Then each crossing in the knot $\mathcal{H}_{\sigma(0)}$ can be replaced (at the cost of further braid eigenvalue factors) with an un-crossing by means of the skein relation corresponding to the characteristic polynomial

$$B_{\sigma(0)\sigma(0)} = \varrho_{\sigma^2(0)}^{\sigma(0)\sigma(0)} I. \quad (6.28)$$

Since the expectation value of a $\sigma(0)$ unknot equals unity (eq. (3.6)),

$$\langle \mathcal{H}_{\sigma(0)} \rangle = \left(\varrho_{\sigma^2(0)}^{\sigma(0)\sigma(0)} \right)^{-w(i, i)} = \exp\left(-i\pi \frac{p+1}{p} (\kappa | \sigma(0)) w(i, i)\right). \quad (6.29)$$

Therefore,

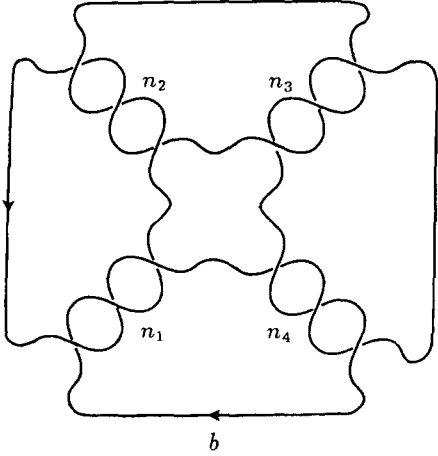
$$\begin{aligned} & \langle \mathcal{L}(\sigma(a_i), \{a_j, j \neq i\}) \rangle \\ &= \exp\left(-i\pi \left[\left(\sum_{j \neq i} w(i, j) q(a_j) \right) + 2w(i, i) q(a_i) + w(i, i) \frac{p+1}{p} (\kappa | \sigma(0)) \right]\right) \\ & \quad \times \langle \mathcal{L}(\{a_i\}) \rangle \end{aligned} \quad (6.30)$$

The explicit values of $(\kappa | \sigma(0))$ are listed in eq. (3.28), and p is the order of σ . We can now use (6.30) to obtain further constraints on a set of graphs of a given type. There will turn out to be enough (linear) equations to completely determine the expectation value of any link-type graph in terms of the links they support. While we do not know these expectation values independently (so that we cannot use these equations to calculate the graphs) we do know their transformation properties (eq. (6.30)) and so can obtain the transformation property of graphs given in eq. (6.17).

First one can insert a spectral decomposition for each crossing in an arbitrary link $\mathcal{L}_{a,b,\dots}$ to get a representation of the link as a sum over planar graphs. At each crossing one can choose to insert an S -channel spectral decomposition so that

$$\mathcal{L} = \frac{(\eta_0^{ap(a)} \eta_0^{bp(b)})^{\mathcal{C}}}{(\chi_q(a) \chi_q(b))^{\mathcal{C}/2}} \sum_{\{s_i\}} \left(\prod_i \sqrt{\chi_q(s_i)} g_{s_i}^{a,b_i} \right) G(a_i, b_i, \dots, \{s_i, \dots\}) \quad (6.31)$$

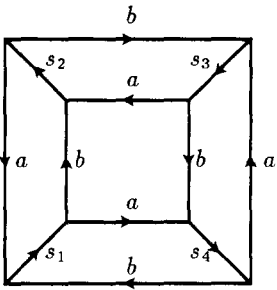
with $\mathcal{C} = \sum |w(i)|$ denoting the number of crossings of the link (alternately, the number of intermediate-channel edges in each graph). Here the indicated graphs only have S -channel twist-type intermediate edges. (While all faces of G with just two edges can be immediately excised, this raises the powers of the braid eigenvalues appearing in (6.31) and potentially introduces a variety of the four channel types, which complicates the argument somewhat.) For example, the family of links



$$\mathcal{L}(a, b; \{n_i\}) = a \quad (6.32)$$

(where each n_i equals the sum of the crossing signs of the neighboring braiding)

has the decomposition

$$\langle \mathcal{L}(a, b; \{n_i\}) \rangle = \sum_{s_1 s_2 s_3 s_4} \left(\prod_{i=1}^4 \sqrt{\frac{\chi_q(s_i)}{\chi_q(a)\chi_q(b)}} (\mathcal{Q}_{s_i}^{ab})^{-n_i} \right) \quad (6.33)$$


If $a \neq b$, then each n_i must be odd so that the sum of the crossing signs between two different components, $\sum_i n_i$, is even. The general cabling result yields, in this case, the equations

$$\mathcal{L}(\sigma(a), b; \{n_i\}) = \exp\left(-i\pi q(b) \left(\sum_i n_i\right)\right) \mathcal{L}(a, b; \{n_i\}) \quad (6.34)$$

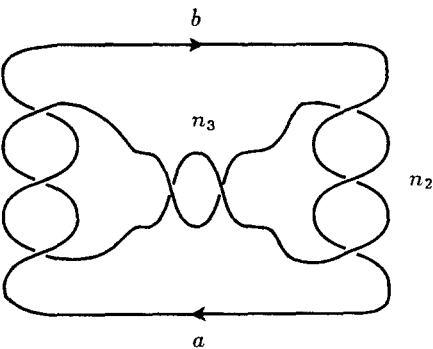
which can be thought of as a set of f^4 linear homogeneous equations (parameterized by the crossing signs n_i) for the f^4 quantities $G(\sigma(a), b; \{\sigma(s_i)\}) - G(a, b; \{s_i\})$, multiplied by certain braid eigenvalues. While the n_i run over all odd integers, the braid polynomial skein relations relate links with different numbers of crossing signs. Given that no unforeseen degeneracies occur this set of equations can be solved only by requiring that eq. (6.17) holds.

Assuming the graph identity in eq. (6.18) yields, via eq. (6.33),

$$\mathcal{L}(a, b; \{n_i\})_{G(N)_K} = \exp\left(-\pi i \Phi(a, b) \sum_i n_i\right) \mathcal{L}(\tilde{a}, \tilde{b}; \{-n_i\})_{G(K)_N} \quad (6.35)$$

as the expected general result for the link in eq. (6.32) (assuming that $a \neq b$ so that $\sum_i n_i$ is even).

Similarly, the class of links

$$\mathcal{L}(a, b; \{n_i\}) = n_1 \quad (6.36)$$


has a decomposition as a sum of graphs of the type in eq. (6.6) via one T -channel and two S -channel insertions so that eq. (6.30) for these links (which is identical to eq. (6.34)) leads to the graph identity in eq. (6.14). Again, assumption of eq. (6.18) for the underlying graph again leads to eq. (6.35).

In general, the rank-level-duality identity for graphs (eq. 6.18) implies the link identity

$$\begin{aligned} \mathcal{L}(\{a_i\})_{G(N)_K} &= \exp\left(\pi i \sum_i w(i, i) r(a_i)\right) \\ &\times \exp\left(-\pi i \sum_{i,j} w(i, j) \Phi(a_i, a_j)\right) \tilde{\mathcal{L}}(\{\tilde{a}_i\})_{G(K)_N}, \\ \Phi(a_i, a_j) &= \begin{cases} r(a_i) r(a_j) / NK & \text{SU}(N)_K \\ 0 & \text{Sp}(N)_K \text{ and } \text{so}(2n+1)_{2k+1}, \end{cases} \end{aligned} \quad (6.37)$$

where $\tilde{\mathcal{L}}$ is the mirror image link of \mathcal{L} . On the basis of the concrete results, and the structure of the known constraint equations, we expect that eq. (6.37) holds for all knots and links.

7. Conclusion

In order to study the exact symmetries of arbitrary Chern–Simons observables we need a systematic reduction of all such observables to known quantities. A previously proposed algorithm involving the reduction of such observables to tetrahedra is ineffective due to the presence of undetermined signs that appear in these reductions. We have found an extension of this algorithm that permits the examination of the symmetries of tetrahedra and certain other Chern–Simons observables. Using this, we have derived the exact form of co-minimal equivalence and rank-level duality for tetrahedra. (This result does not depend on any choice of a system of permutation signs.) For arbitrary link-type graphs (including tetrahedra) we find a set of linear equations; these equations suggest the general form of co-minimal equivalence and rank-level duality for arbitrary link-type graphs. In the case of cominimal equivalence this is confirmed by an argument based on an independent result for links. For rank-level duality we only show that the expected graph result implies the expected link identities (and vice versa). In both cases we exhibit several non-trivial examples consistent with these identities.

For knots these identities require precise control over the permutation signs and conformal dimensions appearing in the braid eigenvalues. Study of these quantities led to an exact formula for the permutation signs in the multiplicity free case (ref. [19]) and the examination of the simple current charges led to the identification of the simple classical origin of these charges (sect. 3).

The most pressing problem raised by this work is to find an effective way of calculating arbitrary (or even just link-type) graphs in a systematic way. The reduction of a knot, link, or graph to a sum of products of tetrahedra (planar or non-planar) is akin to evaluating a lattice partition function, but with an important difference: the Boltzmann weights of a (unitary) lattice partition function are positive definite, but the tetrahedra are not.

Appendix A. Plethysm, permutation signs, and baryons

A.1. YOUNG TABLEAUX AND DYNKIN INDICES

The representations of $SU(N)$, $Sp(N)$, and $so(N)$ that appear on the components and edges of Wilson links and graphs are referred to primarily via Young tableaux. For $SU(N)$, $Sp(N)$, and $so(2n+1)$, the tableau row lengths are given in terms of the Dynkin indices of the highest weight by

$$l_i = \begin{cases} \sum_{j=i}^{\text{rank}\{G\}} a_j & \text{for } G = SU(N) \text{ and } Sp(N) \\ \frac{1}{2}a_n + \sum_{j=i}^{n-1} a_j & \text{for } so(2n+1). \end{cases} \quad (\text{A.1})$$

For $so(2n)$ the natural labels

$$l_i = \begin{cases} \frac{1}{2}(a_n + a_{n-1}) + \sum_{j=i}^{n-2} a_j & \text{for } 1 \leq i \leq n-1 \\ \frac{1}{2}(a_n - a_{n-1}) & \text{for } i = n \end{cases} \quad (\text{A.2})$$

correspond to tableau row lengths for $i = 1, \dots, n-1$. The final tableau row length is given by $|l_n|$. If $l_n \neq 0$, then the representation is characterized by its tableau and the number $\nu \in \{0, 1\}$ defined by $(-1)^\nu = \text{sgn}(a_n - a_{n-1})$. The tableau for a spin-tensor $\{\psi; a\}$ with tensor part a is formed by adjoining a column of n half boxes to the ordinary tableau for a .

For $SU(N)$ and $so(N)$ we refer to *reduced* tableaux. A tableau is reduced if $l_N = 0$ for $SU(N)$ and if $c_1 \leq N - c_1$ for $so(N)$ (the c_i are column lengths). While the tableaux defined in the paragraph above are all reduced, unreduced tableaux appear in the standard procedures for computing tensor products using Young tableaux. In addition, for $so(N)$, the *associate* tableau $\alpha(a)$ of a tableau a only differs from a in that $c_1(\alpha(a)) = N - c_1(a)$. If $\alpha(a) = a$ (requiring $N = 2n$), the representation a is *self-associate*. Since l_n is non-vanishing for these representa-

tions, specification of self-associate representations requires the sign ν in addition to a tableau. All spinors of $SO(2n)$ are self-associate.

Implicit in this paper is the assumption that the tableaux appearing in a level K $G(N)$ theory label integrable representations of $G(N)_K$. This means that $l_1 \leq K$ for $SU(N)$ and $Sp(N)$ and $l_1 + l_2 \leq K$ for $so(N)$.

A.2. BARYON NORMALIZATION AND PERMUTATION SIGN CONSTRAINTS

The crossing constraint $\eta_c^{ab} = \eta_{\rho(a)}^{\rho(c)b}$ in eq. (2.11) follows from comparison of the standard untwisting

$$B_{ab} = Q_c^{ab} \quad (A.3)$$

with the alternate untwisting

$$= \mathcal{F}_a(Q_{\rho(b)}^{\rho(c)a})^{-1} \quad (A.4)$$

where $\mathcal{F}_a = q^{Q(a)/2}$ is the framing factor incurred in undoing the (positive crossing-sign) self-crossing.

We adopt the standard normalization of baryons

$$= \sqrt{\chi_q(a)\chi_q(b)\chi_q(\rho(c))} \quad (A.5)$$

This normalization and the crossing constraint implies a definite relation between any coupling and its dual and leads to the conjugation constraint $\eta_c^{ab} = \eta_{\rho(c)}^{\rho(a)\rho(b)}$ in eq. (2.11). Given a consistent choice of a system of permutation signs there is one sign ω left for the set of four couplings \mathcal{K}_c^{ab} , \mathcal{K}_c^{ba} , \mathcal{K}_{ab}^c , \mathcal{K}_{ba}^c .

In the remainder of this subsection we discuss the origin of the fusion constraint in eq. (2.11). Examination of the U -channel spectral decomposition of the identity shows that

$$\begin{array}{c} \text{---} a \text{---} \\ \text{---} b \text{---} \end{array} = A(a, b) \begin{array}{c} \text{---} a \text{---} \\ \text{---} a \text{---} \\ \uparrow 0 \\ \text{---} b \text{---} \\ \text{---} b \text{---} \end{array} \quad (\text{A.6})$$

where $A(a, b) = \pm 1$. Then

$$\begin{array}{c} \text{---} a \text{---} \\ \text{---} b \text{---} \end{array} = A(a, b) \eta_0^{a\rho(a)} \begin{array}{c} \text{---} a \text{---} \\ \text{---} a \text{---} \\ \uparrow 0 \\ \text{---} b \text{---} \\ \text{---} b \text{---} \end{array} \quad (\text{A.7})$$

If $a = b$ then the sign $A(a, a)$ is intrinsic in the sense that it does not depend on the residual normalization of any couplings, but if $a \neq b$ then $A(a, b)$ depends on the residual normalization of the couplings \mathcal{K}_{0a}^a and \mathcal{K}_b^{0b} . It is natural (though perhaps not necessary) to set the normalization of $\mathcal{K}_{\rho(a)}^{0\rho(a)}$, which couples the ingoing states $|0\rangle \otimes |\rho(a), i\rangle$ to the outgoing states $|\rho(a), i\rangle$, equal to the normalization of \mathcal{K}_a^{0a} . This implies that

$$\begin{array}{c} \text{---} a \text{---} \\ \uparrow 0 \end{array} = \begin{array}{c} \text{---} \rho(a) \text{---} \\ \uparrow 0 \end{array}, \quad (\text{A.8})$$

which, from eqs. (A.6) and (A.7), leads to the equality $A(\rho(a), b) = A(a, b)$.

Similarly, we find that, necessarily,

$$\begin{array}{c} \text{---} b \text{---} \\ \text{---} d \text{---} \\ \uparrow t \\ \text{---} a \text{---} \\ \text{---} c \text{---} \end{array} = R_t \begin{array}{c} \text{---} b \text{---} \\ \text{---} d \text{---} \\ \downarrow \rho(t) \\ \text{---} a \text{---} \\ \text{---} c \text{---} \end{array} \quad (\text{A.9})$$

with $R_t = R_{\rho(t)} = \pm 1$. The couplings that appear on the left- and right-hand side of eq. (A.9) are related by the action of the charge conjugation operator $\mathcal{C}^{\rho(t)t}$: $t \rightarrow \rho(t)$. For example, $\mathcal{K}_b^{\rho(t)d} = \mathcal{C}^{\rho(t)t}(\mathcal{K}_{tb}^d)^{T_1}$ (where T_1 is the partial transpose that effectively raises the indices labeling the states of t). That the right-hand side of eq. (A.9) can be constructed from the left by an odd number of applications of this operator makes it reasonable that a non-trivial sign could appear in eq. (A.9). In this light it is also reasonable that while R_t depends on t it does not depend on the other representations in eq. (A.9). Using these results we will now show that $A(a, a) = 1$ and that $R_t = \eta_0^{t\rho(t)}$.

Using eq. (A.7) we find that

Diagram (A.10) shows a circle with a four-point vertex in the center. The four external legs are labeled 'a' at the top, bottom, left, and right. The two internal legs meeting at the vertex are labeled '0'. This diagram is equal to the product of the coupling $A(a, a)\eta_0^{a\rho(a)}$ and a circle with a vertical line through its center. The two external legs of this circle are labeled 'a' on the left and right, and the vertical line is labeled '0'.

$$\text{Diagram (A.10)} \quad (A.10)$$

Since $R_a^2 = 1$ eq. (A.9) leads to

Diagram (A.11) shows a circle with a four-point vertex in the center. The four external legs are labeled 'a' at the top, bottom, left, and right. The two internal legs meeting at the vertex are labeled '0'. This diagram is equal to the product of the coupling $A(\rho(a), a)\eta_0^{a\rho(a)}$ and a circle with a vertical line through its center. The two external legs of this circle are labeled 'a' on the left and right, and the vertical line is labeled '0'.

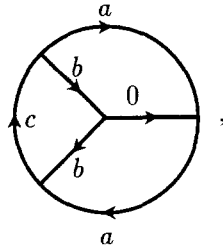
$$\text{Diagram (A.11)} \quad (A.11)$$

These two decompositions, eq. (A.8), and eq. (A.5) imply that

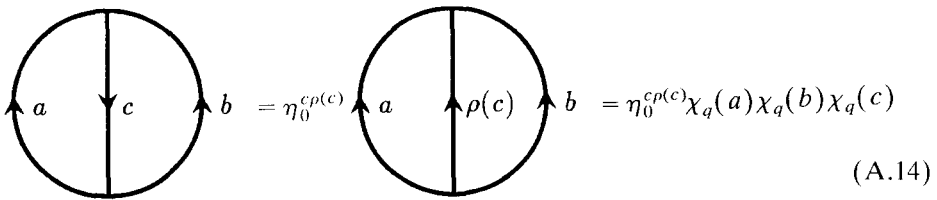
Diagram (A.12) shows a circle with a vertical line through its center. The two external legs are labeled 'a' on the left and right, and the vertical line is labeled '0'. This diagram is equal to the product of the coupling $\eta_0^{a\rho(a)}\chi_q(a)$.

$$\text{Diagram (A.12)} \quad (A.12)$$

which from eq. (A.7) yields $A(a, a) = 1$. If $\rho(a) = a$, then eq. (A.12) holds necessarily, i.e. with any choice of residual couplings. The important point here is simply that (almost necessarily) not all baryons can be normalized to be positive. Since this is the case we have adopted eq. (A.8) in order to put all representations on the same footing. Similar manipulations starting from tetrahedra with only one edge carrying the identity, such as


(A.13)

show that for any a , b , and c , with $c \in a \otimes b$


(A.14)

This result and eq. (A.9) immediately imply that $R_c = \eta_0^{c\rho(c)}$. These baryon signs are responsible for the permutation signs in the dual basis equations in subsect. 2.1. By reversing all the arrows in a baryon, eq. (A.14) implies the fusion constraint $\eta_0^{a\rho(a)}\eta_0^{b\rho(b)} = \eta_0^{c\rho(c)}$ that appears in eq. (2.11).

In this way we obtain the three constraints on the signs in eq. (2.11) from the standard baryon normalization and the apparently innocuous choice of vertical framing.

A.3. THE NATURAL PERMUTATION SIGNS

In the traditional quantum group construction of link and graph invariants [27] finite-dimensional \mathcal{R} -matrices act diagonally on matrices of q -Clebsch–Gordan coefficients, with the diagonal elements given by eq. (2.9), except that the non-crossing symmetric ϵ_c^{ab} appears in place of the crossing-symmetric η_c^{ab} . This difference reflects the fact that the diagram calculus inspired by quantum groups [27] differs from that appropriate to Chern–Simons theory by singling out a

particular direction (a “time” direction). In this sense the Chern–simons graphical calculus is a lagrangian version of the (“hamiltonian”) quantum group graphical calculus. Due to the close correspondence between these two approaches we expect a simple relation between η_c^{ab} and ϵ_c^{ab} , which, in fact, is the case (eq. (2.18)). The quantum group permutation signs can be deduced from (if $a \neq b$ defined via) the matrices of q -Clebsch–Gordan coefficients $(\mathcal{E}_{ab}^c(q))_{ij}^k$ that appear in the tensor product decompositions

$$|c, k\rangle = \sum_{ij} (\mathcal{E}_{ab}^c(q))_{ij}^k |a, i\rangle \otimes |b, j\rangle, \quad (\text{A.15})$$

by means of the identity

$$\mathcal{P}^{ab} \mathcal{E}_c^{ab}(q) = \epsilon_c^{ab} \mathcal{E}_c^{ba}(q^{-1}). \quad (\text{A.16})$$

(Iteration of eq. (A.16) shows immediately that $\epsilon_c^{ab} = \epsilon_c^{ba}$.) The classical limit ($q \rightarrow 1$) shows that ϵ_c^{ab} is simply the (ordinary) group theory permutation sign. While the intrinsic signs ϵ_c^{aa} can just as well be calculated from the classical Clebsch–Gordan coefficients by setting $q = 1$ in eq. (A.16), in the case of ϵ_c^{ab} with $a \neq b$ the powers of q keep track of a natural ordering of states. For example, the fact that in $\text{SU}(3)$ one has $\epsilon_{\begin{smallmatrix} \square & \square \\ \square & \square \end{smallmatrix}} = -1$ may be deduced by applying eq. (A.16) to the embedding of the highest-weight state of $\begin{smallmatrix} \square & \square \\ \square & \square \end{smallmatrix}$ in $\square \otimes \square$

$$|21\rangle = \omega \sqrt{\frac{[2]_q}{[4]_q}} (q^{1/2} |20\rangle \otimes |01\rangle - q^{-1/2} |01\rangle \otimes |20\rangle), \quad (\text{A.17})$$

where the states are labeled by Dynkin indices and $\omega = \pm 1$ remains unfixed after imposing $\langle 21|21\rangle = 1$. The permutation sign is *intrinsic* in the sense that it originates in the relative sign between the leading term and its permutation in such decompositions and is independent of ω . The same procedure, when applied to the embeddings of the highest-weight state of $\begin{smallmatrix} \square & \square \\ \square & \square \end{smallmatrix}$ in the tensor product $\square \otimes \square$ and in its permutation $\square \otimes \square$, respectively,

$$\begin{aligned} |11\rangle &= \omega_1 \frac{1}{\sqrt{[3]_q}} \left(\sqrt{[2]_q} q^{1/4} |20\rangle \otimes |-11\rangle - q^{-1/2} |01\rangle \otimes |10\rangle \right) \\ |11\rangle &= \omega_2 \frac{1}{\sqrt{[3]_q}} \left(q^{1/2} |10\rangle \otimes |01\rangle - \sqrt{[2]_q} q^{-1/4} |-11\rangle \otimes |20\rangle \right) \end{aligned} \quad (\text{A.18})$$

yields $\epsilon_{\begin{smallmatrix} \square & \square \\ \square & \square \end{smallmatrix}} = -\omega_1 \omega_2$. We have defined the normalization sign to be the sign of the highest power of q . Given this it seems natural to take a uniform sign of the

square root when imposing $\langle 11|11\rangle = 1$ so that $\omega_1 = \omega_2$. The permutation sign then indicates the relative sign between the leading state (as ordered by powers of q) and its permutation (with the inverse power of q).

In all cases, once a system of permutation signs is chosen, we have exactly one sign choice ω remaining for each $c \in a \otimes b$. This corresponds to the residual normalization remaining for Chern–Simons vertices.

These natural – or structural – permutation signs can be obtained without having to compute the couplings $\mathcal{E}_{ab}^c(q)$. The explicit formula eq. (2.16) for the multiplicity-free case is derived in ref. [19] and allows rapid evaluation of ϵ_c^{ab} in these cases. While this is useful for many purposes, a spurious dependence on row lengths sometimes appears which would actually disappear if one knew how to impose the condition of no multiplicities in general.

Since the fusion ring is a quotient of the tensor ring by a certain ideal, the terms ϕ_c remaining in the fusion of ϕ_a and ϕ_b inherit the permutation sign from the tensor ring. This is unambiguous if c appears in the tensor product $a \otimes b$ with multiplicity one, or if the fusion multiplicity equals the tensor multiplicity. There remains a problem if the fusion ring multiplicity is less than the tensor ring multiplicity (but not zero), which we call the problem of *reduced* fusion multiplicities. In such cases, the known algorithms [29] for computing the fusion product do not indicate whether symmetric or anti-symmetric terms are removed from the product; they only yield the sum of symmetric and anti-symmetric multiplicities

$$N_{ab}^{\pm c} = N_{ab}^{+c} + N_{ab}^{-c}. \quad (\text{A.19})$$

We have found two ways to obtain information about $N_{ab}^{\pm c}$ (via Chern–Simons theory itself). First, by expanding a singly-twisted unknot (or its mirror image) with a spectral decomposition of the crossing, two equations for the difference $N_{ab}^{+c} - N_{ab}^{-c}$ are obtained. While this (allied with the single-multiplicity formula (2.18)) is effective in many situations, it seems possible that more than two separate cases of reduced multiplicities could appear in a fusion product. Second, the result in eq. (6.30), which embodies the exact symmetry under co-minimal equivalence, often correlates reduced multiplicities in one fusion product with non-reduced multiplicities in co-minimal fusion products.

A.4. CO-MINIMAL EQUIVALENCE AND PERMUTATION SIGNS

The application of this Chern–Simons argument (in eq. (3.18)–(3.29)) uses this latter approach (i.e. that via eq. (6.30)) to demonstrate the braid eigenvalue relations directly in almost all cases, including that of reduced multiplicities. In addition, the identities in eqs. (3.12) and (3.13) for $\text{SU}(N)$, and eq. (3.26) for the remaining groups, follow in the case of no multiplicity directly from the level formula. One reason that this is possible is that the leading sign in the case of

multiplicities (i.e. that spurious sign given by the level formula to all copies of a representation in the case of multiplicity) satisfies the single multiplicity equations without further constraint so that no spurious row length dependencies appear in these single multiplicity formulae.

In contrast, in the similar situation for rank-level duality, the analogous level formula relation contains a complicated dependence on row lengths. This dependence would disappear if one knew in general how to impose the condition of no multiplicity. It is at this point that the complementary approach via plethysm comes to the rescue since it is not restricted to the multiplicity-free case.

A.5. THE RANK-LEVEL DUALITY OF PERMUTATION SIGNS FROM PLETHYSM

The Littlewood–Richardson product of tableau characters is denoted by

$$\text{char}(a) \cdot \text{char}(b) = \sum \text{char}(c).$$

If the character of any tableau whose first column length exceeds a given integer N ($N \geq 2$) is set to zero identically, then this product is just the tensor product of (purely covariant tableaux of) $\text{GL}(N)$. If, in addition, the character of any tableau whose first column length equals N is identified with the character of the tableau obtained by removing this first column of length N , then this product is just the tensor product of $\text{SU}(N)$. The product of characters needed for $\text{Sp}(N)$ and $\text{SO}(N)$ is defined in terms of the Littlewood–Richardson product by

$$\text{char}(a) \times \text{char}(b) = \sum_d \text{char}((a/d) \cdot (b/d)). \quad (\text{A.20})$$

Here (a/d) denotes the sum of all tableaux a_d such that $a_d \cdot d$ contains a . Define $\Gamma(a_d) = r(d)$ (i.e. the number of boxes in the tableau d). The tensor product of $\text{Sp}(N)$ and $\text{SO}(N)$ (tensor) representations is obtained from eq. (A.20) by imposing certain character identities (that are more involved than in the $\text{SU}(N)$ case [28]). Then, for $c \in a \otimes b$, the quantity $\Gamma(c)$ gives the number of contractions of tensor indices needed to obtain c in the tensor product $a \otimes b$.

The permutation signs for $\text{SU}(N)$, $\text{Sp}(N)$, and $\text{SO}(2n+1)$ may all be obtained from $\text{GL}(N)$, via

$$\begin{aligned} \epsilon_c^{ab}{}_{\text{SU}(N)} &= \epsilon_c^{ab}{}_{\text{GL}(N)}, \\ \epsilon_c^{ab}{}_{\text{Sp}(N)} &= e^{i\pi\Gamma(c)} \epsilon_c^{a_d b_d}{}_{\text{GL}(N)}, \\ \epsilon_c^{ab}{}_{\text{so}(2n+1)} &= \epsilon_c^{a_d b_d}{}_{\text{GL}(N)}, \end{aligned} \quad (\text{A.21})$$

where $a_d \in (a/d)$, $b_d \in (b/d)$ and $c \in a_d \cdot b_d$.

Under rank-level duality a representation c in the decomposition of $a \otimes a$ is often paired by transposition (4.1) with $\tilde{c} \in \tilde{a} \otimes \tilde{a}$ (the case $\Delta_c^{aa} = 0$ in eq. (4.3)). For all these cases we can use a standard result of the calculus of plethysm to show that [3]

$$\epsilon_s^{aa} \epsilon_{\tilde{s}}^{\tilde{a}\tilde{a}} = e^{i\pi r(a)} \quad \text{GL}(N) \quad (\text{A.22})$$

Here we give the proof of this result. We will denote the operation of plethysm between two tableaux by a star:

$$a * \mu \quad (\text{A.23})$$

denotes the plethysm of the tableau a by the tableau μ . We will be interested in the case $\mu = \square$ (which corresponds to the symmetric product of a) and $\mu = \begin{smallmatrix} \square \\ \square \end{smallmatrix}$ (the anti-symmetric product). A classic theorem of plethysm states that:

Theorem. (p. 54 of ref. [30])

Given that $a * \mu = \Sigma s$,

if $r(a)$ is even then $\tilde{a} * \mu = \Sigma \tilde{s}$, while

if $r(a)$ is odd then $\tilde{a} * \tilde{\mu} = \Sigma \tilde{s}$.

Proof of eq. (A.22): Consider the product $\epsilon_s^{aa} \epsilon_{\tilde{s}}^{\tilde{a}\tilde{a}}$. First assume that s is in the symmetric part of $a \otimes a$ so that $\mu = \square$. Then, if $r(a)$ is even the above theorem states that \tilde{s} is also in the symmetric part of $\tilde{a} \otimes \tilde{a}$. Therefore $\epsilon_s^{aa} \epsilon_{\tilde{s}}^{\tilde{a}\tilde{a}} = 1 = e^{i\pi r(a)}$, since $r(a)$ is even. If $r(a)$ is odd then the above theorem states that \tilde{s} is in the anti-symmetric part of $\tilde{a} \otimes \tilde{a}$, so that $\epsilon_s^{aa} \epsilon_{\tilde{s}}^{\tilde{a}\tilde{a}} = -1 = e^{i\pi r(a)}$. Similarly, assuming that s is in the anti-symmetric part, so that $\mu = \begin{smallmatrix} \square \\ \square \end{smallmatrix}$, means that \tilde{s} is also in the anti-symmetric part if $r(a)$ is even, but is in the symmetric part if $r(a)$ is odd and in either case $\epsilon_s^{aa} \epsilon_{\tilde{s}}^{\tilde{a}\tilde{a}} = e^{i\pi r(a)}$. Therefore, eq. (A.22) holds for all a . \square

For $\text{Sp}(N)_K$ the fusion rule identity $N_{ab}^c = N_{\tilde{a}\tilde{b}}^{\tilde{c}}$, eq. (A.21), and the $\text{GL}(N)$ result (A.22) yield the rank-level permutation sign transformation in the intrinsic case $a = b$, except in the case of reduced multiplicities. With $\Gamma(s)$ denoting the number of contractions in the tensor product,

$$(\epsilon_s^{aa})_{\text{Sp}(N)_K} (\epsilon_{\tilde{s}}^{\tilde{a}\tilde{a}})_{\text{Sp}(K)_N} = (\epsilon_s^{a_d a_d})_{\text{GL}(N)} e^{i\pi \Gamma(s)} (\epsilon_{\tilde{s}}^{\tilde{a}_d \tilde{a}_d})_{\text{GL}(K)} e^{i\pi \Gamma(\tilde{s})}, \quad (\text{A.24})$$

where $s \in a_d \cdot a_d$ and $\tilde{s} \in \tilde{a}_d \cdot \tilde{a}_d$. Using the fact that $\Gamma(s) = \Gamma(\tilde{s})$ and eq. (A.22) we find that

$$(\epsilon_s^{aa})_{\text{Sp}(N)_K} (\epsilon_{\tilde{s}}^{\tilde{a}\tilde{a}})_{\text{Sp}(K)_N} = e^{i\pi r(a_d)} = e^{i\pi(r(a) - r(d))}. \quad (\text{A.25})$$

But $r(d) = \Gamma(s)$, and we find that

$$(\epsilon_s^{aa})_{\text{Sp}(N)_K} (\epsilon_{\tilde{s}}^{\tilde{a}\tilde{a}})_{\text{Sp}(K)_N} = e^{i\pi(r(a) - \Gamma(s))} \quad (\text{A.26})$$

holds in all cases (given that s and \tilde{s} do not appear with reduced multiplicities). Note that eq. (A.22) implies that if the tensor and fusion multiplicities are equal then

$$N_{aa}^{+c} - N_{aa}^{-c} = e^{i\pi r(a)} (N_{\tilde{a}\tilde{a}}^{+\tilde{c}} - N_{\tilde{a}\tilde{a}}^{-\tilde{c}}),$$

so that $N_{aa}^{+c} = N_{\tilde{a}\tilde{a}}^{\pm\tilde{c}}$ as $r(a)$ is even or odd. Then we can extend the definition of the transposition map so that eq. (A.26) holds both in the single and full multiplicity cases.

The identical result follows for the $SO(2n+1)_{2k+1}$ fusion rule by similar reasoning as follows. From the fusion rule identity $N_{ab}^c = N_{\tilde{a}\tilde{b}}^{\sigma^{a\tilde{b}}(\tilde{c})}$ we know that ϵ_s^{aa} is paired with $\epsilon_{\tilde{s}}^{\tilde{a}\tilde{a}}$ if $\Delta_s^{aa} = 0 \bmod 2$ and with $\epsilon_{\sigma(\tilde{s})}^{\tilde{a}\tilde{a}}$ if $\Delta_s^{aa} = 1 \bmod 2$. In the first case

$$(\epsilon_s^{aa})_{so(2n+1)_{2k+1}} (\epsilon_{\tilde{s}}^{\tilde{a}\tilde{a}})_{so(2k+1)_{2n+1}} = (\epsilon_s^{a_d a_d})_{GL(N)} (\epsilon_{\tilde{s}}^{\tilde{a}_d \tilde{a}_d})_{GL(K)} \quad (A.27)$$

and exactly the same arguments show that

$$(\epsilon_s^{aa})_{so(2n+1)_{2k+1}} (\epsilon_{\tilde{s}}^{\tilde{a}\tilde{a}})_{so(2k+1)_{2n+1}} = e^{i\pi(r(a) - \Gamma(s))} \quad (A.28)$$

holds (apart from the case of reduced multiplicities). If $\Delta_s^{aa} = 2r(a) - r(s) = 1 \bmod 2$, then $r(s)$ is odd. This can only occur if the reduction rule has been used in producing $r(s)$ via eq. (A.20). Since $\epsilon_s^{aa} = \epsilon_{\alpha(s)}^{aa}$ and $\widetilde{\alpha(s)} = \sigma(\tilde{s})$, where $\alpha(s)$ is the associate tableau of the representation s , we have

$$(\epsilon_s^{aa})_{so(2n+1)_{2k+1}} (\epsilon_{\sigma(\tilde{s})}^{\tilde{a}\tilde{a}})_{so(2k+1)_{2n+1}} = (\epsilon_{\alpha(s)}^{a_d a_d})_{GL(N)} \left(\epsilon_{\widetilde{\alpha(s)}}^{\tilde{a}_d \tilde{a}_d} \right)_{GL(K)} = e^{i\pi r(a_d)}, \quad (A.29)$$

where $\alpha(s) \in a_d \otimes a_d$ and $\widetilde{\alpha(s)} \in \tilde{a}_d \otimes \tilde{a}_d$. Then $r(a_d) = r(a) - \Gamma(s)$, so that

$$(\epsilon_s^{aa})_{so(2n+1)_{2k+1}} (\epsilon_{\sigma^{\Delta_s^{aa}}(\tilde{s})}^{\tilde{a}\tilde{a}})_{so(2k+1)_{2n+1}} = e^{i\pi(r(a) - \Gamma(s))} \quad (A.30)$$

holds in all cases (except those involving reduced multiplicities).

If $\Delta_s^{aa} = 0$ then eq. (A.22) is exactly the $SU(N)$ result for this case. If $\Delta_s^{aa} \neq 0$ but $\Omega^{aa}(s) = 0$, which means that the *unreduced* tableau s'' has $l_1'' \leq K$, then the tableau for $\sigma^{\Delta_s^{aa}}(\tilde{s})$ is just that for \tilde{s}'' so that

$$(\epsilon_s^{aa})_{SU(N)_K} (\epsilon_{\sigma^{\Delta_s^{aa}}(\tilde{s})}^{\tilde{a}\tilde{a}})_{SU(K)_N} = (\epsilon_{s''}^{aa})_{GL(N)} \left(\epsilon_{\widetilde{s''}}^{\tilde{a}\tilde{a}} \right)_{GL(K)} = e^{i\pi r(a)} \quad (\text{for } \Omega^{aa}(s) = 0) \quad (A.31)$$

holds in all (non-reduced multiplicity) cases. A consideration of various specific cases suggests that, in fact,

$$\epsilon_s^{aa} \epsilon_{\sigma^{-aa}(\bar{s})}^{\bar{a}\bar{a}} = e^{i\pi(r(a) + \Omega^{aa}(s))} \quad (\text{A.32})$$

for $SU(N)_K$.

Since $\eta_s^{aa} = \epsilon_s^{aa}$ all these results hold directly for the Chern–Simons (single and full multiplicity) permutation signs as well.

While all these tensor ring permutation sign results are inherited by the fusion ring in the indicated situations, to obtain results for the reduced multiplicity case for all groups and the $\Omega^{aa}(s) \neq 0$ cases for $SU(N)$ we must appeal to the Chern–Simons knot-based arguments. For cominimal equivalence the cabling argument yields a complete confirmation that the single multiplicity case extends to all cases with multiplicity (whether reduced or not). For rank–level duality we can only use the figure-eight and its complex conjugate to get two equations for the reduced multiplicity signs. While this only implies that the single multiplicity case necessarily extends to fusion products with at most two reduced multiplicity terms, this represents an infinite class of non-trivial examples, on which to base the general result.

References

- [1] E. Witten, Commun. Math. Phys. 121 (1989) 351; Nucl. Phys. B322 (1989) 629; B330 (1990) 285
- [2] G. Moore and N. Seiberg, Phys. Lett. B220 (1989) 422
- [3] S. Naculich, H. Riggs and H. Schnitzer, Phys. Lett. B246 (1990) 417
- [4] J. Fuchs and D. Gepner, Nucl. Phys. B294 (1987) 30
- [5] D. Bernard, Nucl. Phys. B288 (1987) 628
- [6] I. Frenkel, in Lie Algebras and related topics, Lecture Notes in Mathematics, 933, ed. D. Winter (Springer, Berlin, 1982) p. 71;
- M. Jimbo and T. Miwa, in Adv. Stud. Pure Math. 4 (1984) 97; 6 (1985) 17;
- M. Jimbo, T. Miwa and M. Okado, Lett. Math. Phys. 14 (1987) 123
- [7] E. Mlawer, S. Naculich, H. Riggs and H. Schnitzer, Nucl. Phys. B352 (1991) 863; A quantum generated symmetry of conformal and topological field theory, in Quantum field theory, statistical mechanics, quantum groups, and topology, ed. T. Curtright et al. (World Scientific, Singapore, 1992) p. 218
- [8] A. Kuniba and T. Nakanishi, Level–rank duality in fusion RSOS models, Proc. Int. Coll. on Modern quantum field theory, TIFR, Bombay, India, 1990;
- A. Kuniba, T. Nakanishi and J. Suzuki, Nucl. Phys. B356 (1991) 750
- [9] H. Saleur and D. Altschüler, Nucl. Phys. B354 (1991) 579
- [10] A. Schellekens and S. Yankielowicz, Int. J. Mod. Phys. A5 (1990) 2903;
- K. Intriligator, Nucl. Phys. B332 (1990) 541
- [11] J. Fuchs, Quantum dimensions, CERN preprint, CERN-TH.6156-91, July 1991
- [12] J. Fuchs and P. van Driel, J. Math. Phys. 31 (1990) 1770; Nucl. Phys. B346 (1991) 632
- [13] D. Altschüler, M. Bauer and C. Itzykson, Commun. Math. Phys. 132 (1990) 349
- [14] S. Martin, Nucl. Phys. B338 (1990) 244
- [15] R. Dijkgraaf and E. Witten, Commun. Math. Phys. 129 (1990) 393

- [16] V. Drinfeld, Quantum groups, in *Proc. Int. Congress of Mathematicians* (Berkeley, California, 1986) 789;
M. Jimbo, *Lett. Math. Phys.* 10 (1985) 63
- [17] E. Witten, The central charge in three dimensions, in *The physics and mathematics of strings*, ed. L. Brink (World Scientific, Singapore, 1990) p. 530
- [18] L.H. Kauffman, *Trans. Amer. Math. Soc.* 318 (1990) 417; *Knots and physics*, (World Scientific, Singapore, 1991)
- [19] S. Naculich, H. Riggs and H. Schnitzer, in preparation
- [20] J. Fuchs, *Commun. Math. Phys.* 136 (1991) 345
- [21] D. Gepner, *Phys. Lett. B*222 (1989) 207;
W. Lerche, C. Vafa and N. Warner, *Nucl. Phys. B*324 (1989) 427;
C. Ahn and M. Walton, *Phys. Rev. D*41 (1990) 2558
- [22] A. Schellekens and S. Yankielowicz, *Nucl. Phys. B*327 (1989) 673; *B*334 (1990) 67
- [23] F. Lemire and J. Patera, *J. Math. Phys.* 21 (1980) 2026
- [24] S. Naculich and H. Schnitzer, *Phys. Lett. B*244 (1990) 235; *Nucl. Phys. B*347 (1990) 687;
T. Nakanishi and A. Tsuchiya, *Commun. Math. Phys.* 144 (1992) 351
- [25] L. Alvarez-Gaumé, C. Gomez and G. Sierra, *Nucl. Phys. B*330 (1990) 347
- [26] N. Chair and C.-J. Zhu, *Int. J. Mod. Phys. A*6 (1991) 3571
- [27] N. Reshetikhin, Quantized universal enveloping algebras, the Yang–Baxter equation, and invariants of links, LOMI preprints E-4-87 and E-17-87, 1987
- [28] R. King, *J. Math. Phys.* 12 (1971) 1588
- [29] M. Walton, *Phys. Lett. B*241 (1990) 365, *Nucl. Phys. B*340 (1990) 777;
M. Spiegelglas, *Phys. Lett. B*245 (1990) 169;
P. Furlan, A. Ganchev and V. Petkova, *Nucl. Phys. B*343 (1990) 205;
J. Fuchs and P. van Driel, *Nucl. Phys. B*346 (1990) 632;
V. Kac, to appear
- [30] B. Wybourne, *Symmetry principles and atomic spectroscopy* (John Wiley and Sons, New York, 1970)